Quaternary International xxx (xxxx) xxx

Contents lists available at ScienceDirect

Quaternary International

journal homepage: www.elsevier.com/locate/quaint

Neolithic livestock practices in high mountain areas: A multi-proxy study of pastoral enclosures of Molleres II (Eastern Pyrenees)

Valentina Pescini [a,*], Arnau Carbonell [a], Lídia Colominas [a], Natalia Égüez [b,c], Alfredo Mayoral [a,d], Josep Maria Palet [a]

[a] Institut Català d'Arqueologia Clàssica, Plaça d'en Rovellat, s/n, 43003, Tarragona, Spain
[b] Archaeological Micromorphology and Biomarkers -AMBI Lab, Instituto Universitario de Bio-Orgánica Antonio González, Universidad de La Laguna, 38206, Tenerife, Spain
[c] Department of Anthropology, University of California, Davis, CA, USA
[d] Université Clermont Auvergne, CNRS, GEOLAB, F-63000, Clermont-Ferrand, France

ARTICLE INFO

Keywords:
Animal husbandry
Palaeoenvironment
Geo- and Bio markers
Fire use
Neolithic
Middle Ages

ABSTRACT

This paper presents the results of the archaeological and palaeoenvironmental investigation carried out at Molleres II site located at 2.425 m a.s.l. in the area of Puigpedrós-Malniu (Meranges, La Cerdanya, Eastern Pyrenees). A high-resolution multi-proxy research is proposed combining landscape archaeology, soil micromorphology, anthracology, biomolecular analysis, and radiocarbon dating. This work allowed us to characterize the site's functionality, providing new insight into the occupation dynamics of high mountain spaces starting from the Neolithic onwards. Based on this research Molleres II has been interpreted as a complex and wide open-air site built up by the end of the Middle Neolithic (3636–2701 cal. BC) and consisting of large enclosures entirely dedicated to seasonal animal husbandry and located at an exceptionally high altitude. These unique settings make the site a primer for this period and in the Eastern Pyrenees, revealing the considerable intensity of the animal presence since the Prehistory in these uplands.

Following the Neolithic, a second phase of more intense occupation likely occurred during Middle Ages (1179–1434 cal. AD). However, the animal presence in this mountain sector had never been exhausted, even in other historical periods. Palaeoenvironmental data also suggest that such intense and long-term animal presence and possibly fire use could be at the origin of stable grassland-dominated environments and open landscapes maintained almost continuously until nowadays.

1. Introduction

Landscape research in Pyrenean high mountain environments carried out in recent decades has highlighted the intensity and antiquity of the processes of occupation in these areas, documented since the Early Neolithic, around the 5th millennium BC (Ejarque, 2013; Gassiot et al., 2014; Gassiot, 2016, Orengo et al. 2014; Palet et al., 2013, 2014, 2017, 2019, 2022a, 2022b). These researches show that long-term occupation and exploitation of these environments have transformed them over time, constituting at present valuable cultural landscapes.

Following the GIAP-ICAC research on Mountain Cultural Landscapes (Ejarque, 2013; Ejarque et al., 2010; Palet et al., 2014, 2017, 2019, 2022), since 2018, multi-scale and interdisciplinary research has been developed in the Pyrenean axial mountain range in *La Cerdanya* (Palet et al., 2020). With similar approaches and objectives, these researches focus on the historical process of occupation and exploitation of high mountain cultural landscapes and the role of societies in shaping these high mountain environments. The study is therefore approached from the Landscape Archaeology theoretical and practical framework, based on the integration and correlation of multi-proxy data adapted in high mountain spaces (Rendu, 2003; Orengo, 2010; Ejarque, 2013; Palet et al., 2014; Walsh et al., 2014).

This paper presents the research results developed in Molleres II, a complex livestock site located in Puigpedrós-Malniu (Meranges, Cerdanya) at 2.425 m a.s.l. Several studies in the Eastern Pyrenees have shown that anthropization and landscape transformation intensified throughout the Neolithic period, becoming more intense in the Late Neolithic (Rendu, 2003; Gassiot et al., 2014; Palet et al., 2017, 2022a).

* Corresponding author.
E-mail address: vpescini@icac.cat (V. Pescini).

https://doi.org/10.1016/j.quaint.2023.04.008
Received 11 October 2022; Received in revised form 24 February 2023; Accepted 19 April 2023

However, despite this evidence, few archaeological sites are documented from this period, being mainly located in caves or shelters because of the climatic and erosive conditions of these high mountain environments.

Here we present a Neolithic deposit in an open area, which is extraordinary in high mountain areas. To obtain as much information as possible about this exceptional site, the study proposes a high-resolution multi-proxy analysis combining archaeological and environmental data on an intra-site scale, with the application of anthracological, micromorphological, lipid and carbon and deuterium stable isotope analyses together with radiocarbon dating. This approach has allowed us to characterize the site's functionality and demonstrate the importance of summer pastures already in the Neolithic.

2. Study area

Molleres II site (2.425 m a.s.l.; UTM ETRS89: x399071, y4702651/ Geographic coordinate system: 42.469578 N, 1.772193 E) is located in the Puigpedrós-Malniu mountain range within the Cerdanya region (Eastern Pyrenees) (Fig. 1).

The study area has an extremely simple geology, as it is exclusively composed of the Palaeozoic granodiorites of the Puigpedrós Massif, which is structurally part of the Axial section of the Pyrenees range (IGME, 1994). The area was heavily glaciated during the Last Glacial Maximum and the Lateglacial, and most of the superficial formations derive from reworked glacial and periglacial deposits or directly from regolith and granodiorite weathering. Geomorphologically, the site is located in the head of a small thalweg in the shoulder just below the Coll de Molleres pass, in a more or less regular slope facing south/southeast with abundant sparse boulders of granodiorite of variable size, typical of mountain granitic landscapes. Holocene slope dynamics seem to have been dominated by low-intensity periglacial slope processes involving freeze-and-thaw and snow accumulation, such as gelifraction, formation of nivation niches or diffuse and concentrated runoff reworking the regolith. These processes have led to the formation of a colluvial layer draping all this upper slope area, in general thin (<30–50 cm) but with locally thicker accumulations following the local microtopographic variations. This colluvial layer does not seem particularly affected by solifluction or gelifluction and is currently well-covered by grasses. The area's soils are developed directly on such colluvium or the granodioritic regolith. They are generally very thin and with very limited evolution and could be classified as leptosols or regosols. Vegetation surrounding Molleres II is mainly composed of irregular and open mountain pine (*Pinus uncinata* R. ex DC.) population associated with scattered shrubs (i.e., *Juniper communis* subsp. *alpine* Čelak) formations (Ninot et al., 2007; Vigo, 2009). The herbaceous layer (currently grazed by small herds of cows and horses) consists of mat grass (*Nardus stricta* L.) and other plants typical of mountain pastures (*Trifolium alpinum* L., *Ranunculus pyrenaeus* L., *Plantago alpina* L. etc.). The climate is typical of high Mediterranean mountains, with very cold and snowy winters and cool and stormy summers without a significant summer drought.

3. Material and methods

3.1. Archaeological survey, test pit digging and radiocarbon dating

To retrieve archaeological data in the high mountain area of *la Cerdanya*, a complete cartographic database in a georeferenced GIS environment was used. Topographic maps (1:5000), high-resolution multi-temporal orthophotos (0.25 m/pixel), slope maps (<25%), land cover maps (LCM), digital elevation models (DEM), and LiDAR image processing were employed to locate anthropogenic elements using photointerpretation procedures and plan survey operations (Orengo, 2010; Palet et al., 2017). The areas of highest archaeological

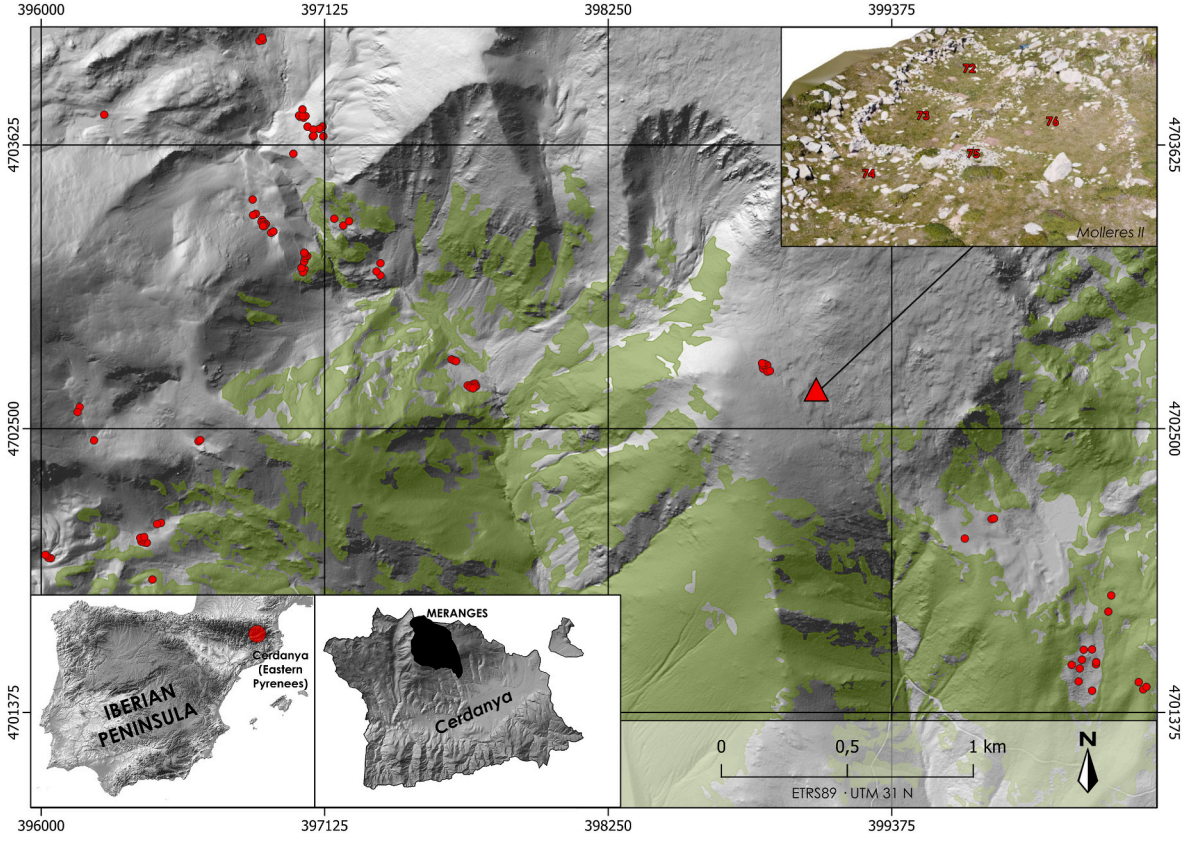

Fig. 1. Study area location and orthophoto of Molleres II site. Red circles refer to further archaeological structures localized during archaeological survey carried out on the Puigpedrós-Malniu mountain range.

significance were then defined from this first diagnosis. The pre-inventory was supported by the QFIELD software, an interactive database that enables real-time updating of the inventory database, facilitating, standardizing, and systematizing the capture of georeferenced data. All data were stored on a portable device (smartphones, tablets, or laptops) equipped with onboard GPS and GIS software. With this approach and technology, it was possible to localize the site of Molleres II which, subsequently, was subjected to a specific archaeological survey to complement and verify the photointerpretation results. This was done by incorporating localized structures into vector layers linked to the geo-referenced database. During the survey, all the structures' characteristics were registered (dimensions, shape of the stone walls, preservation issues, presence of a sedimentary deposit for a subsequent excavation etc.). Once the most suitable structures for excavation were identified, shovel test pits were carried out. In high mountain environments the resources and time available for excavation are limited. Therefore, diagnostic testing is the most effective method to recover archaeological information (i.e., structure typology, construction, use and abandonment phases, chronologies etc.). The strategy behind the location of the test pits was aimed, on the one hand, at finding the best-preserved sediments as highlands are often subjected to erosion processes, possibly deleting archaeological stratigraphies. On the other hand, the choice was directed to those sediments directly related to the structure to be excavated. Once the best places were selected and marked, the second operation was opening the pits to be excavated by cutting the grass. This last was kept aside and subsequently relocated after the closure of the pits to avoid leaving open depressions, which, in addition to being dangerous, could constitute trigger points for surface erosion. The excavation methodology followed the standard stratigraphic procedures and was carried out with a trowel and/or a pickaxe. All the sediment from the different stratigraphic units was dry sieved (2 mm mesh); the recovered archaeological material (i.e., pottery) was recorded and stored in plastic bags. The stratigraphic sequences in high mountain areas tend to provide sparse archaeological material due to the physicochemical characteristics of the soils (very acidic, often subject to erosion phenomena). In these circumstances, obtaining a chronostratigraphic framework can therefore be challenging. Yet, charcoal fragments, which are instead relatively common in these contexts, represent valuable remains to develop chronological models. Charcoals to be dated were selected based on their location along the stratification, their sizes (between 2 and 4 mm, avoiding possible wind-transported fragments) and their taphonomy (avoiding rolled or eroded fragments). Finally, when possible, the plant species of the fragments were identified. AMS radiocarbon dating of charcoal fragments was obtained at the Poznań Radiocarbon Laboratory. OxCal v4.4.2 (Bronk Ramsey, 2020) software was used to calibrate the ^{14}C dates in calendar years, based on the IntCal 20 database (Reimer et al., 2020).

Geolocation techniques, such as photogrammetry and drones, were also used to record archaeological excavations. The drone-based image acquisition was conducted with a Mavic Air 2. Considering its weight (570 g), this model is very suitable for work in high mountains. Using photogrammetric processes with Agisoft Metashape professional software, all the images from a single flight were merged together to produce a single georeferenced orthophoto. These techniques allowed us a fast and precise acquisition of high-resolution models and planimetry of the whole site.

3.2. Anthracology

Samples for anthracological analysis were collected in all the three excavated test pits. All the excavated layers of the structures were carefully dry-sieved during the archaeological campaign using a 2 mm mesh sieve. In addition, a total of 4L of sediments were sampled for each charcoal-rich layer (i.e., SU72104, SU73104 and SU76104).

The 4L of sediment collected during the campaign was subsequently floated at the Catalan Institute of Classical Archaeology (ICAC) of Tarragona: meshes of 4, 2, 1 and 0,25 mm were used to extract charcoal fragments and other charred plant macro-remains (i.e., seeds, chaff, stems, branches etc.).

Several studies have demonstrated how the analysis of 2 and 4 mm meshes is sufficient to obtain a realistic anthracological analysis (Kabukcu and Chabal, 2021; Chabal, 1997); however, at Molleres II, since the presence of well-preserved charcoal remains were scarce it was decided to analyse even the finest mesh (1 mm). In general, in anthracology, the analysis of this mesh is to be avoided as the taxonomic identification is difficult and takes time due to the small size of the fragments but could be valuable for the study of shrubs (Asouti and Austin, 2005).

The anthracological analysis was carried out both at the Laboratory of Bioarchaeology of the ICAC and at the Laboratory of Environmental Archaeology and History (LASA) of the University of Genoa (Italy).

Charcoal identification has been obtained using reflected light microscopy, both bright- and dark-field (Olympus BX51 and Nikon Optiphot 100) using magnifications of x50, x100, x200 and x500. A stereomicroscope (LEICA M80) with magnifications from x7.5 to x60 was used to detect charred plant macro-remains retained in the 1 mm mesh.

The totality of $\geq$2 mm charcoal fragments have been analyzed; instead, around 25 remains between 2 and 1 mm have been observed according to the low specific richness of these contexts.

Charcoal identification was based on anatomical features described in atlases of wood anatomy (Greguss, 1959; Schweingruber, 1990), Websites (Wood anatomy, InsideWood Database, Xylem database and Digital Plant Atlas) and was supported by the reference collection of modern charcoal remains stored at the LASA. Botanical nomenclature follows The Plant List (TPL) and the following specific criteria particularly referred to *Pinus* fragments. Anatomically, the identification of the species belonging to the European mountain pine complex (Hamerník and Musil, 2007; Sokołowska et al., 2021) is difficult as diagnostic traits are very similar and hybridization is frequent; in anthracology this difficulty is even greater given the poorly preserved small fragments available for taxonomic identification (Schweingruber, 1990; Allué et al., 2018; Figueiral and Carcaillet 2005). In the present study, the distinction between the different mountain pine species followed the criteria proposed by Euba (2008) (e.g., width of growth rings, position of the resiniferous channels etc.) but above all the local biogeographical setting. Indeed, since Molleres II is located at a fairly high altitude (>2.000 m a.s.l.), thus corresponding to the alpine zone, the probability that charcoal remains corresponded to *Pinus* tp. *uncinata* (Ramond ex DC.) is greater (Quézel and Médail, 2003; Vidaković, 1991; Folch, R., 1986; Ninot et al., 2017). Thus, only when all the above characteristics were present *Pinus* fragments have been classified as *Pinus* tp. *uncinata* (Ramond ex DC.). When the identification stopped at the *genus* level this was followed by sp. (e.g., *Pinus* sp.); if the anatomical diagnostic characteristics were too unclear to identify the *genus*, it was preferred to report it prefacing the names with the abbreviation cf. (e.g., cf. *Pinus*). The term "indeterminate" has been attributed to those fragments too damaged to study their anatomy (e.g., "vitrified" charcoal fragments, deriving from the fusion and homogenization of wood charcoal cell walls, Courty et al., 2020; McParland et al., 2010). Finally, charcoal remains showing bark were counted and analyzed to identify the cutting season.

3.3. Soil micromorphology

Sediment monoliths were plastered and extracted from S072 and S076 for micromorphological analysis. A single monolith was retrieved from S076 (28–77 cm, SU76101 to SU76105), and two partly overlapping monoliths from S072 (8–34 and 28–60 cm, SU72102 to SU72105) (see also Supplementary material #1). Once in the laboratory plaster was cut, and the unnecessary thickness of the monoliths was

removed by hand to improve the subsequent impregnation process with synthetic resin. A total of 13 standard-size blocks (13,5 × 6,5 cm) were cut from the impregnated monoliths, with overlappings of c. 50% between each block and the following. They were used to produce 30 μm covered micromorphological thin sections following the standard procedure with BrotLab equipment (Guilloré, 1980) in the IPHES facilities (Tarragona, Sp.). Resulting thin sections were assessed visually and analyzed from macro-to-microscale under a binocular stereoscopic microscope (x7,5 to x50) and a Zeiss Axioscope petrographic microscope (x16 to x400) using cross-polarized light (XPL), plane polarized light (PPL), and oblique incident light (OIL) and in a few cases blue light fluorescence (BLF). An external micro camera (Spot Insight) was used to take microphotographs and measurements. Mineral components and their alteration were described following petrography references (MacKenzie et al., 1982; Delvigne, 1998; Loaiza et al., 2015). Qualitative and semi-quantitative systematic descriptions of micromorphological features were performed in standardized description sheets based on reference works (Bullock et al., 1985; Loaiza et al., 2015; Stoops, 2021), and relevant elements were compiled in summarized descriptions. Interpretations were proposed following international up-to-date literature (Nicosia and Stoops, 2017; Macphail and Goldberg, 2018; Stoops et al., 2018; Verrecchia and Trombino, 2021).

3.4. Lipid extraction, analysis and quantification

Ten sediment samples (MOLL1-MOLL10) were processed for lipid extraction, identification and quantification at AMBI Lab (La Laguna, Spain). Between 2 and 3g of each sediment sample were dried at 60 °C over 48h and then homogenized using an agate mortar. Before extractions, all glassware and glass wool was placed in a muffle oven at 550 °C for 3 h to eliminate any possible organic compounds. Protocols for the total lipid extract (TLE) and fraction separation of *n*-alkanes, aromatics and alcohols compounds via silica gel column chromatography were followed as in Jambrina-Enríquez et al. (2018), Leierer et al. (2019), Connolly et al. (2019) and Tomé et al. (2022).

A second TLE extraction was performed for saponification to obtain the sterols, stanols and bile acids (Elhmmali et al., 1997, modified see Padrón Herrera, 2021). Detailed extraction protocol is available in Supplementary material #2.

Common indexes developed for helping the environmental interpretation of occurring wax *n*-alkanes abundances were used: the carbon preference index (CPI), average chain length (ACL) and P- aqueous (Paq). CPI measures the relative abundance of odd over even carbon, whereas ACL is the weighted average of the various carbon chain lengths (Duan and He, 2011; Bush and McInerney, 2015). Paq was first proposed by Ficken et al. (2000) to separate submerged/floating aquatic macrophyte inputs from emergent and terrestrial plant input to sediments.

The *n*-alkane distribution was calculated according to the Carbon Preference Index (CPI) using the Bray and Evans equation (1961) (Eq. 1):

$$CPI_{25} = [(\Sigma C_{25-33odd} / \Sigma C_{24-32even}) + (\Sigma C_{25-C33odd} / \Sigma C_{26-C34even})] \times 0.5$$

The average chain length (ACL) was calculated following the recommendation of Freeman and Pancost (2014). For total *n*-alkanes we used the C_{15}–C_{33} interval (Eq. 2):

$$ACL_{15\text{-}33total} = \Sigma(Ci \times [Ci]) / \Sigma[Ci];\ 15 \leq i \leq 33$$

The value [Ci] is the concentration of the *n*-alkane with i carbon atoms.

Paq is defined as follows:

$$Paq = (C23 + C25)/(C23 + C25 + C29 + C31)$$

Different ratios for the identification of faecal remains were used:

Ratio 1. Based on Prost et al. (2017). A value greater than 0.7 confirms the presence of excrement; between 0.3 and 0.7, it does not allow confirming or ruling out the presence of excrement; less than 0.3 rules out the presence of excrement.

$$(5\beta\text{-}estigmastanol + epi\text{-}5\beta\text{-}estigmastanol) / (5\alpha\text{-}estigmastanol + 5\beta\text{-}estigmasaanol + epi\text{-}5\beta\text{-}estigmastanol)$$

Ratio 2. Based on Prost et al. (2017). Indicates whether the faecal matter analyzed belongs to pig, human or herbivore. A value < 29% indicates that the faecal matter derives from a herbivorous animal; >65% confirms the human origin, and between the previous values, of pig. The presence of certain bile acids is also considered to determine the origin source.

$$coprostanol / coprostanol + 5\beta\text{-}estigmastanol\ x100$$

Ratio 3. Based on Shillito et al. (2011). It is used to confirm whether the faecal matter derives from pigs/humans or ruminant animals (>1 equals omnivore; <1 equivalent to herbivore).

$$(coprostanol + epicoprostanol) / (5\beta\text{-}estigmastanol + epi\text{-}5\beta\text{-}estigmastanol)$$

Ratio 4. Based on Evershed and Bethell (1996). Proposed as a helpful index to differentiate human faecal deposition from that of ruminants (sheep and cows). Values > 1.5 are indicative of human-sourced pollution.

5β- Cholestanol:5β- Stigmastanol

Ratio 5. By Leeming et al. (1997). Used to estimate the relative contribution of different faecal sources. Values > 73% related solely to human contamination and <38% only from herbivores.

$$(coprostanol)/(coprostanol+5\beta\text{-}stigmastanol) \times 100.$$

If the signal is mixed, the proportion of herbivore input could be calculated following:

% herbivore derived contribution = (73−Y) × 2.86 (Leeming et al., 1997; Shillito et al., 2011).

3.5. Compound-specific carbon and deuterium isotope analysis

Carbon isotope analysis by GC-IRMS was performed at AMBI Lab using a Thermo Scientific Isotope Ratio Mass Spectrometer Delta V Advantaged coupled to a GC Trace1310 through a Conflo IV interfaced with a temperature converter GC Isolink II. Samples were injected by using MultiMode injector (MMI) in splitless mode, with the temperature increasing from 79 °C (held 0.5 min) to 325 °C (held 3min) at a rate 10 °C·s^{-1} and finally to 350 °C (held 3min) at 14 °C·s^{-1}. The GC was fitted with a Trace Gold 5-MS (Thermo Scientific) fused silica capillary column (30 m length x 0.25 mm i.d., 0.25 μm film thickness). Helium was used as the carrier gas at a flow rate set at 1.5 mL min^{-1}. The combustion reactor temperature was maintained at 1000 °C. The temperature programme comprised a 2 min isothermal period at 70 °C increasing to 140 °C (held 2 min) at a rate of 12 °C·min^{-1}, followed by an increase period to 320 °C (held 15 min) at 3 °C·min^{-1}. Data acquisition and processing were carried out using the Isodat 3.0 software (Thermo Scientific). $\delta^{13}C$ and $\delta^{2}H$ values were standardised to VPDB (Vienna Pee Dee Belemnite) and Vienna Standard Mean Ocean Water (VSMOW) scale using an *n*-alkane Schiemmelmann type A6 mixture (n-C_{16} to n-C_{30}). Certificate of analysis indicates that data for *n*-alkane Schimmelmann type A6 mixture has a precision of ±0.05‰ for δ13C and ±1.5‰ for $\delta^{2}H$. Reproducibility was better than ±0.5‰ for carbon isotope measurements and better than ±5.0‰ for hydrogen isotope measurements.

4. Results

4.1. Archaeological results

The Molleres II site was located through photo interpretation and

inventoried during the 2018 survey (Palet et al., 2020). It is an archaeological site with 5 structures (S) located on a slope (Fig. 2). They are irregular enclosures made of granodiorite boulders. Three of them (S072, S073, S074) appear as terraces that follow the slope's orientation (north-south). The largest (S076) is on the north-east side of the ensemble. A smaller quadrangular structure named S075, approximately 4 × 4 m, was also documented between S073 and S076.

During the 2020 campaign, a total of three diagnostic test pits on S072, S073, and S076 were carried out, recording the stratigraphic succession until the natural substrate. The test pits were located in those more consistent and preserved sedimentation zones and in correspondence with the different stone walls constituting the various structures to obtain the archaeological relation between the walls and the stratigraphy.

Structure 072 is an enclosure (13.7 × 11.4m) with a semi-oval shape built on the slope at the top of the site. Despite its slope, the enclosure exhibits significant sedimentation. A 1 × 2 m test pit was carried out against the southern wall (SU72120), on the inside of the structure, providing a stratigraphic sequence 56–64 cm deep that leaned against the wall for all this depth (Fig. 2). The superficial Stratigraphic Unit (SU) (72101), was a layer of light brown disaggregated soil thick between 5 and 6 cm followed by a darker and compacted layer about 10–20 cm thick (SU72102). Sporadic presence of macrocharcoals was noted in this layer, and again in the SU72103, a brown compact layer (clayey sands) about 10–15 cm thick. This layer covered SU72104, a slightly more organic stratum with a greyer colour about 25 cm thick: it constitutes the first layer of accumulation of the wall structure (SU72120) which in turn sets itself on the weathered bedrock (SU72105) (see also Supplementary material #1). No artefacts (ceramic or lithic) were recovered.

Structure 073 is an enclosure located between S072 (upper-north) and S074 (lower-south); it is polygonal in shape (12.5 × 13m) and with appropriate sedimentation despite the slope of the surrounding terrain. A 1 × 2 m test pit was made inside the structure, oriented north-south, next to the walls (SU73120) separating this enclosure from S075 and S074. It provided a sequence 54-49 cm deep that leaned against the wall for all this depth (Fig. 2). Similarly to S072, the stratigraphic sequence revealed a layer of sedimentation (SU73103) just below the destruction of the structure (SU73102, characterized by large stones). Twelve common coarse pottery of reduced firing fragments were located in these layers (SU73102-73103) which could be associated with S075, the rectangular and very small structure whose perimeter walls are set to those pertaining to S073. This material is small and devoid of significant diagnostic features; no more archaeological remains were recovered in these layers except for some charcoal fragments.

Structure 076 is a large (18.2 × 14.6m) enclosure located east of S072, S073 and S074. A test pit of 1.5 × 1.5 m was dug on the southern wall (SU76120) of the structure, providing a stratigraphic sequence 52–70 cm deep that leaned against the wall for all this depth (Fig. 2). In the most superficial part of the pit's section two layers (SU76101 and SU76102) were identified: both were characterized by macrocharcoals while SU76102 contained a pottery fragment with an oxidized and completely disintegrated ceramic paste. No more archaeological materials were recovered during the excavation of the pit. Below, SU76103 was a stratum about 2–20 cm thick and slightly more clayey that reached its maximum thickness in the eastern sector of the test pit. This layer covered SU76104, a black-brown compacted layer about 2–5 cm thick and rich in charcoal fragments that obliterated the weathered bedrock (SU76105) on which the wall structure (SU76120) was set.

The three test pits allowed us to attest to the construction technique of the enclosure walls. Built of dry stone, the walls present granite

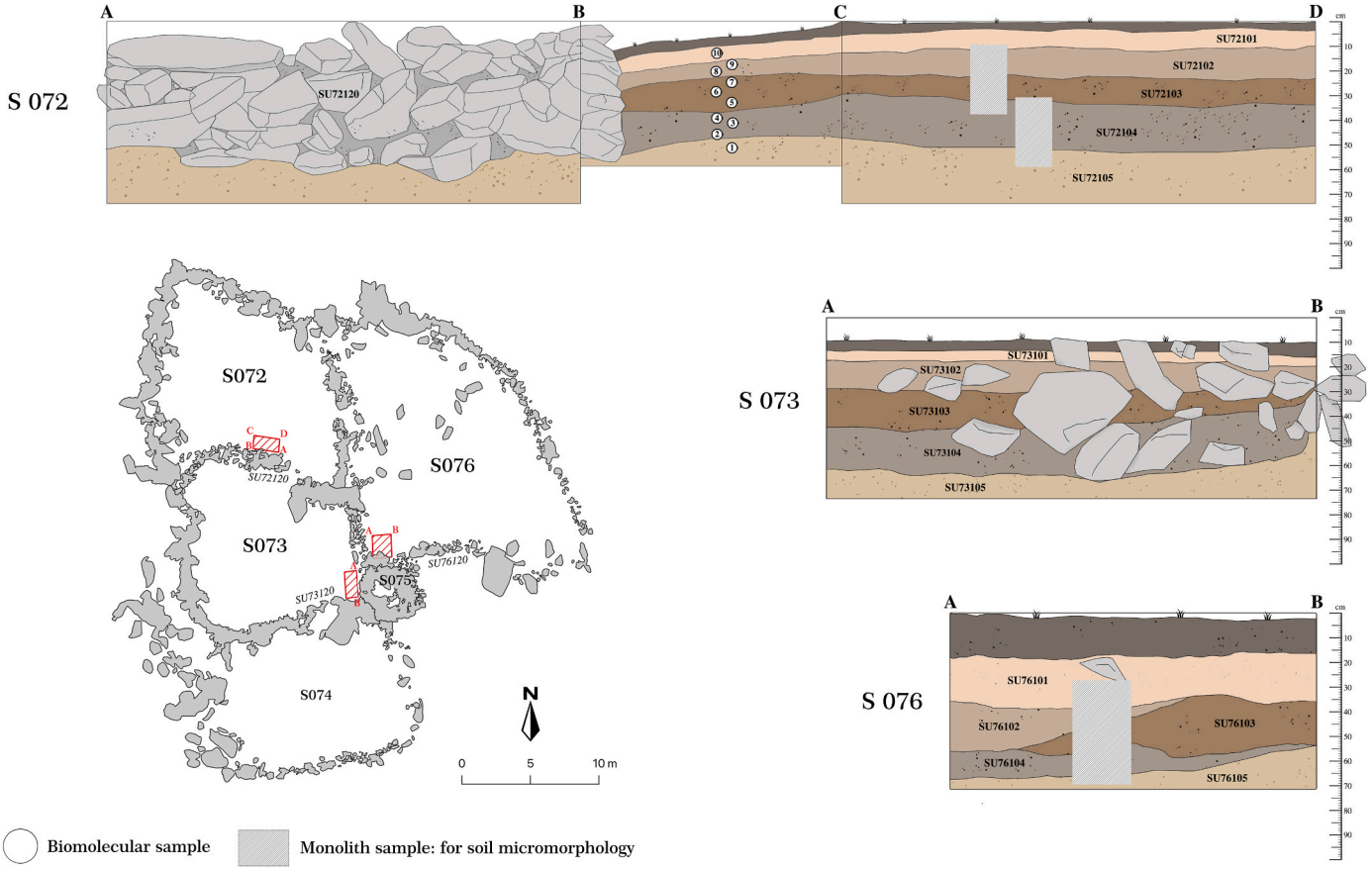

Fig. 2. Planimetry of Molleres II site with the stratigraphic profiles of archaeological structures. The numbering of the bimolecular samples follows the collection technique, from the bottom up to avoid possible contamination from the upper layers during the sampling.

boulders of large (e.g., 24 × 16 cm) and medium size (e.g., 12 × 6 cm), with a height of about 60 cm and a width of approximately 80–100 cm, with a wall seen inside. This was especially visible in S072, while in S076, the granite boulders were slightly displaced inwards. In the case of S073, boulders associated with the very first layers were documented below the base of the hut (S075), located right next to the test pit. The three walls present the same construction technique from stacked dry stone.

4.2. Radiocarbon

A total of six AMS radiocarbon dates were obtained; results are presented in Table 1.

The sporadic presence of macrocharcoals in S072 allowed the dating of two SUs. The SU72104 shows a chronology of 2923–2701 cal. BC (Table 1: date Poz-130426), and the SU72102 is dated in 1179–1278 cal. AD (Table 1: date Poz-130278).

Structure 073 was dated from the compacted SU73104 above the natural substrate (SU73105) to date the use of the first phase related to the structure. The results again show a chronological frame corresponding to the beginning of the Late Neolithic (3283 - 2906 cal. BC) (Table 1: date Poz-130279).

In relation to structure 076, a greater amount of charcoal remains was detected in the SU76104, related to the first accumulation layer connected to S076: two radiocarbon dating analyses were performed. The first corresponds to the transition between the 7th and the 6th mil. BC (6219 - 5926 cal. BC) (Table 1: date Poz-130428) while the second ones to the Middle Neolithic (3636 - 3380 cal. BC) (Table 1: date Poz-133848). This second dating is more likely, in comparison with the other dates obtained at Molleres II and in the broader framework of the chronology of occupation of the Pyrenean mountains (Ejarque, 2013; Gassiot et al., 2014; Orengo et al. 2014). The SU76102, which contained an oxidized ceramic paste that was disintegrated entirely, was also dated, showing a Middle Ages chronology (1318–1434 cal. AD) (Table 1: Poz-130427) that fits with the chronological frame detected in S072.

Two chronological ranges are thus evident at Molleres II: an older one dating back to the transition between the Middle and Late Neolithic documented in the three structures (S072, S073, S076) and the other to the Middle Ages, attested in S072 and S076.

4.3. Anthracological results

A total of 225 fragments ≥1 mm were analyzed. Charcoal fragments were generally scarce, although a slight increase has been identified in the deeper layers. Since no particular differences were identified between the floated or dry sieved charcoal remains nor between the three different meshes, the results were merged and presented in Fig. 3 as percentage graphs expressed for each excavated layer.

A total of three *taxa* were identified. Pine is the most abundant *taxon* (76,5%), and at least 44,9% has been identified as *Pinus* tp. *uncinata*. Some of these fragments could be related to pine long/dwarf shoots, probably derived from burning pine needles. Sporadic fragments likely attributable to fern specimens have also been observed. The fragments' small size and high vitrification do not allow a precise taxonomic identification, although some similarities are found with *Equisetum* and *Osmunda* (See also Supplementary material #3). The carefulness in identifying these *taxa* is also due to the habitual distribution range of these plants, which generally do not reach such high altitudes.

No particular differences between the two identified chronological phases (Middle/Late Neolithic and Middle Ages) have been detected, as pine remains the most abundant plant in all the excavated structures. It was impossible to specify the felling season as none of the analyzed fragments had bark; instead, pith was present in two fragments of pine (both in SU76102) and in all the analyzed herbaceous *taxa* (ferns). The latter are finally those that have been most subject to vitrification processes.

4.4. Micromorphological results

4.4.1. General micromorphological features and main pedo-sedimentary processes

Pedosedimentary sequences contained by both archaeological structures share several micromorphological features, summarized below. Key relevant features are shown in Fig. 4 and semi-quantitatively represented in Fig. 5. Stratigraphic units and boundaries are generally diffuse at the microscopic scale, although the major SUs can be distinguished. The groundmass-related distribution pattern is complex, ranging from fine to equal; and single-to double-spaced enaulic, including mineral grains, soil granules, and larger welded granules or crumbs, typical of surface horizons rich in organic matter (Stoops and Mees, 2018). The C/F relation (limit fixed at 20 μm) is highly variable between samples and within a single thin section, although it ranges between 10% and 50%. Porosity is mainly made of complex packing voids between the soil particles (10–40% of the TS, typically 20–25%). Other voids, such as small cracks, vughs, and small channels (200–400 μm) with remains of rootlets are also abundant but represent a negligible part of the soil porosity. Larger (400 μm to millimetric) channels, which can be attributed to earthworms' activity (Kooistra and Pulleman, 2018), are less abundant and appear, in general, cracked and degraded. This fact, combined with the absence of passage features, suggests continuous bioturbation of the profile. The resulting microstructure can be divided into a primary microgranular structure, with a mixture of smooth, rounded granules of different sizes (40–100 μm), sometimes as loose infillings, but most frequently in coalescent masses or welded in larger crumbs/granules with variable degrees of aggregation and separation (Fig. 4-A). Considering the size, homogeneity, and aspect of microgranules, it can be interpreted as an excremental microstructure (Verrecchia and Trombino, 2021). The secondary microstructure is a complex mixture of well-rounded granular, mamillated, and rugged crumbly aggregates (200 μm to 5 mm) resulting of the fusion of finer granules, with different degrees of aggregation and separation. Among them, large fecal pellets of earthworms present a more rounded and/or elongated shape and less porous texture, and less content in organic matter. Locally this structure is more welded and resembles a pseudo-porphyric microstructure. The high number of excremental features from microfauna of different sizes, with different degrees of ageing and maturation, whereas passage features are poorly preserved, suggests a permanent churning of soil structure (Kooistra and Pulleman,

Table 1
AMS Radiocarbon results and calibrated ages with probability of some selected charcoal particles (taxon ID: *Pinus* tp *uncinata* or *Pinus* sp.) from different Stratigraphic Units.

Lab code	S	Typology	SU	^{14}C yr. BP	(1σ) ^{14}C yr cal. BC/AD	(2σ) ^{14}C cal. yr. BC/AD	Archaeological interpretation
Poz-130428	076	Undeter.	104	7190 ± 50	6078–5996 BC	6219–5926 BC	Palaeosoil before occupation?
Poz-133848	076	Enclosure	104(b)	4755 ± 35	3630–3520 BC	3636–3380 BC	Occupation level
Poz-130279	073	Enclosure	105	4390 ± 35	3078–2926 BC	3283–2906 BC	Occupation level
Poz-130426	072	Enclosure	104	4255 ± 35	2910–2786 BC	2923–2701 BC	Occupation level
Poz-130278	072	Enclosure	102	805 ± 30	1224–1263 AD	1179–1278 AD	Occupation level
Poz-130427	076	Enclosure	102	550 ± 30	1328–1423 AD	1318–1434 AD	Occupation level

S= Structure; SU=Stratigraphic Unit.

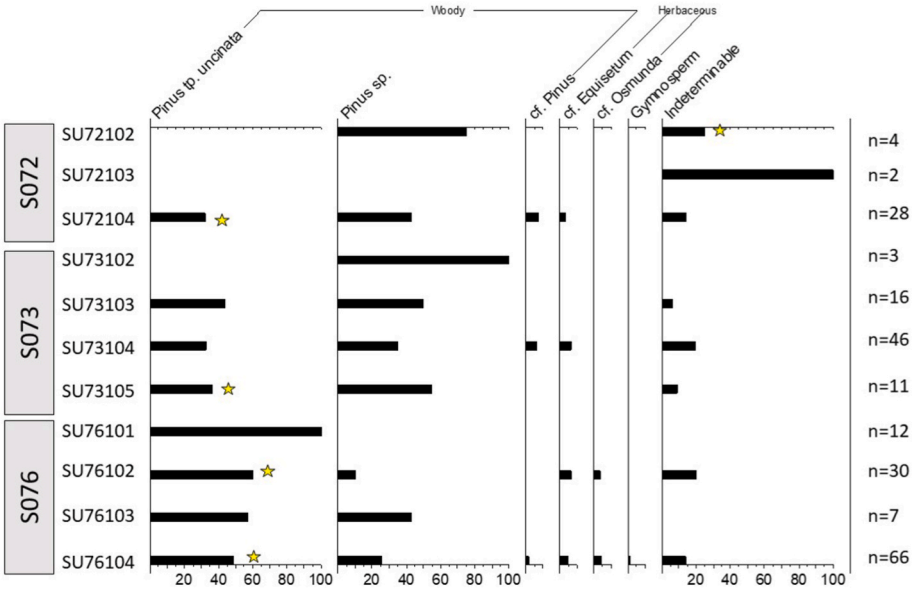

Fig. 3. Anthracological percentage diagram. Results are presented per each investigated structures and according to stratigraphic succession. The yellow star refers to the charcoal fragments subjected to radiocarbon dating.

2018). Frost features are not preserved despite the altitude and the seasonal freezing of the soil, reinforcing this idea. Together, all these features indicate that both pedosedimentary sequences are subject to very intense and constant pedo-and bioturbation by roots and soil fauna during the relatively short growing season in high altitudes (Gerasimova and Lebedeva, 2018), partly blurring the stratigraphy of the sequence. These observations are highly consistent with the macroscopic field evidence, with poorly defined layers relatively homogeneous in terms of color, texture, and structure, very abundant rootlets forming a thick mat in almost all the stratigraphy, and the presence of small earthworms and other microfauna.

The coarse fraction is abundant, consistently with high mountain soils and sediments derived from granodiroritic regolith. It includes abundant lithogenic particles, mainly granodioritic rock fragments of variable sizes, most often sandy to gravelly, with sometimes millimetric particles typically angular and irregular. Single-grain individual minerals are also abundant, including quartz, feldspar (mainly plagioclase), biotite and hornblende, with angular shapes and variable sizes from silts to very coarse sand or gravel. The number and grain-size of these lithogenic components are here interpreted as a proxy of detrital inputs from nearby areas or weathering/reworking of the structures themselves. Weathering preferentially affects the assemblage's weakest minerals, i.e., hornblendes and biotites, which can be strongly weathered, rarely feldspars, and almost never quartz. This suggests a context of reduced weathering (Delvigne, 1998), although significant differences between samples exist (Fig. 5). Weathering products are mainly iron oxides/hydroxides and whitish clays (sericite), and are likely due to changes in redox and slow pedoplasmation (Stoops and Schaefer, 2018; Vepraskas et al., 2018). Phytoliths are also extremely abundant in all the samples (e.g., Fig. 4-I and 4-J), with a random and homogeneous distribution in the micromass, consistent with grasslands environments in a rather acid soil environment (Kaczorek et al., 2018). However, their sustained presence in all the sequence makes it difficult to use them as a proxy of palaeoenvironmental changes without a specific study.

The micromass is quite humic, with light to dark brown color, rarely reddish or sepia. It is dotted with silt-sized organic debris and microcharcoal (<20 μm) and includes many reddish, brown, or black organic microdebris and microcharcoal. This, together with organic gel and pigments with the same colors, gives the micromass a cloudy aspect. Ubiquitous oblong to acicular microliths/cristallites form a sericitic cristallitic B-fabric. The intricate admixture of mineral and organic micromatter in both sequences suggests that they can be interpreted as thick organo-mineral A horizons (Gerasimova and Lebedeva, 2018), as also pointed out by the microstructure, the common presence of fresh rootlet remains or the faunal features (see above). Other organic material includes extremely abundant microcharcoal (<125 μm) and quite frequently macrocharcoal (>125 μm, sometimes reaching millimetric sizes, Fig. 4-B). The latter present in general angular and fragile shapes and are considered traces of in-situ burning of woody or herbaceous plants (Deák et al., 2017). Other remains of organic tissues in different states of aging are also present in small amounts throughout the sequence, and their number is inversely proportional to bioturbation and organic matter maturation. Small diffuse Fe and Mn mottles, sometimes evolving to small and diffuse weakly to moderately impregnated nodules and more rarely to larger and strongly impregnated Fe-Mn nodules, are present in small numbers in all the pedosedimentary sequence. Their size, number, and degree of impregnation are used as an indicator of redox conditions linked to the length and intensity of temporary water saturations (Vepraskas et al., 2018).

4.4.2. *Selected diagnostic micromorphological features of S076 and S072*

S076. The deepest unit of this structure (SU76105) shows the presence of an "inorganic" micromass in amounts up to 50% (Fig. 5). This "inorganic" yellowish micromass is characterized by the total absence of organic remains, organic debris dotting, microcharcoal and organic gel or pigments, and a reduced amount of phytoliths. As a result, it has a clayey limpid micromass with lighter colors and a clear sericitic cristallitic B-Fabric (Fig. 4-F & G). This micromass is present in aggregates with different shapes or in larger areas very clearly differentiated from the organic-rich micromass of the rest of the sequence or even as coatings of larger mineral grains. The lack of macrocharcoals and very limited bio- and pedoturbation in SU76105 suggest the absence of local fires and very limited soil activity/disturbance. Larger grain-size of rock particles (granules to coarse gravels), more pronounced minerals weathering, and more notable redox features indicate the proximity of the bedrock and water stagnation at the base of the profile (Vepraskas et al., 2018) certainly after the formation of SU76105, perhaps due to local drainage deterioration after construction of S076.

Overlying layer (SU76104), the first layer of infilling of the archaeological structure and dated c. 3500 cal. BC (Fig. 5), presents far less aggregates with inorganic micromass, redox features, and minerals weathering, but traces of bioturbation are more intense. This change is

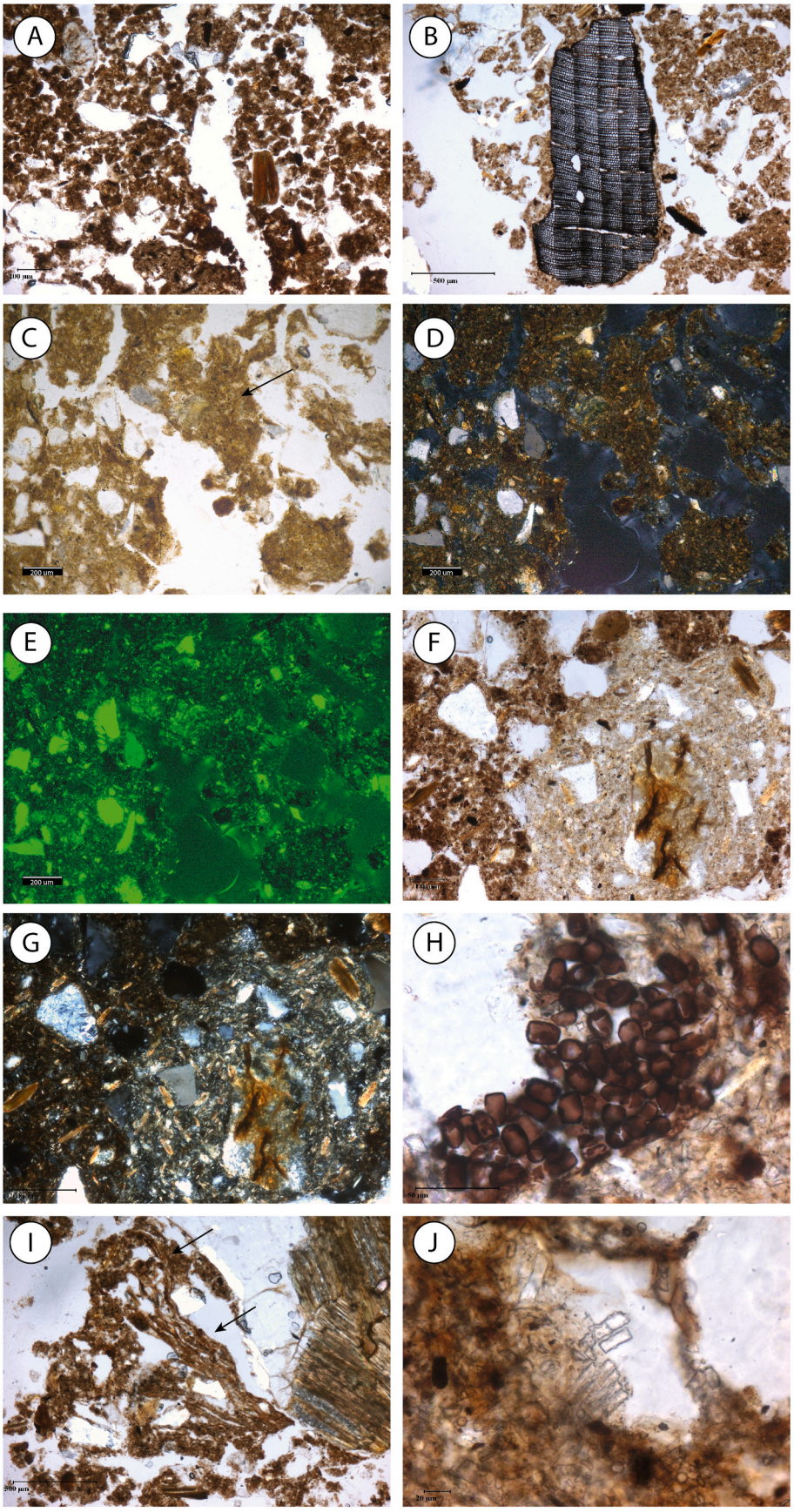

Fig. 4. Relevant micromorphological features of pedo-sedimentary sequences of S076 and S072. A) Channel in a microgranular (excremental) microstructure. Note the organic-rich micromass and the variable ageing and coalescence degree of granules to form larger granules or crumbles (SU76103, PPL); B) Large macrocharcoal of woody material, note the 6 growth rings. Note also in the microstructure the different degrees of coalescence and welding of small microgranules to form larger aggregates (SU76104, PPL); C) Aggregate (arrow) with crystalline and amorphous phosphate pedofeatures (translucent to brownish yellow) as nodules (SU72104, PPL); D) Same in XPL, note greyish-yellowish colors and partial extinction of phosphatic areas. Note the cristallitic sericitic B-Fabric; E) Same in BLF, note the light green fluorescence of the phosphatic pedofeatures compared to dark groundmass and highly fluorescent quartz grains; F) Aggregate of "inorganic" micromass. Note the sharp contrast between the limpid, mineral micromass and the organic-rich, dark brown micromass structured in microgranules dotted by extremely abundant dark debris (SU76105, PPL); G) Same aggregate in XPL, note the much clearer sericitic cristallitic B-Fabric pattern in absence of organic matter; H) Cluster of spores of Sporormiella-type coprophilous fungi (SU72105, PPL); I) Fragment of microlayered micromass (black arrows; SU72105, PPL); J) Abundant phytoliths visible in the micromass (SU76103, PPL).

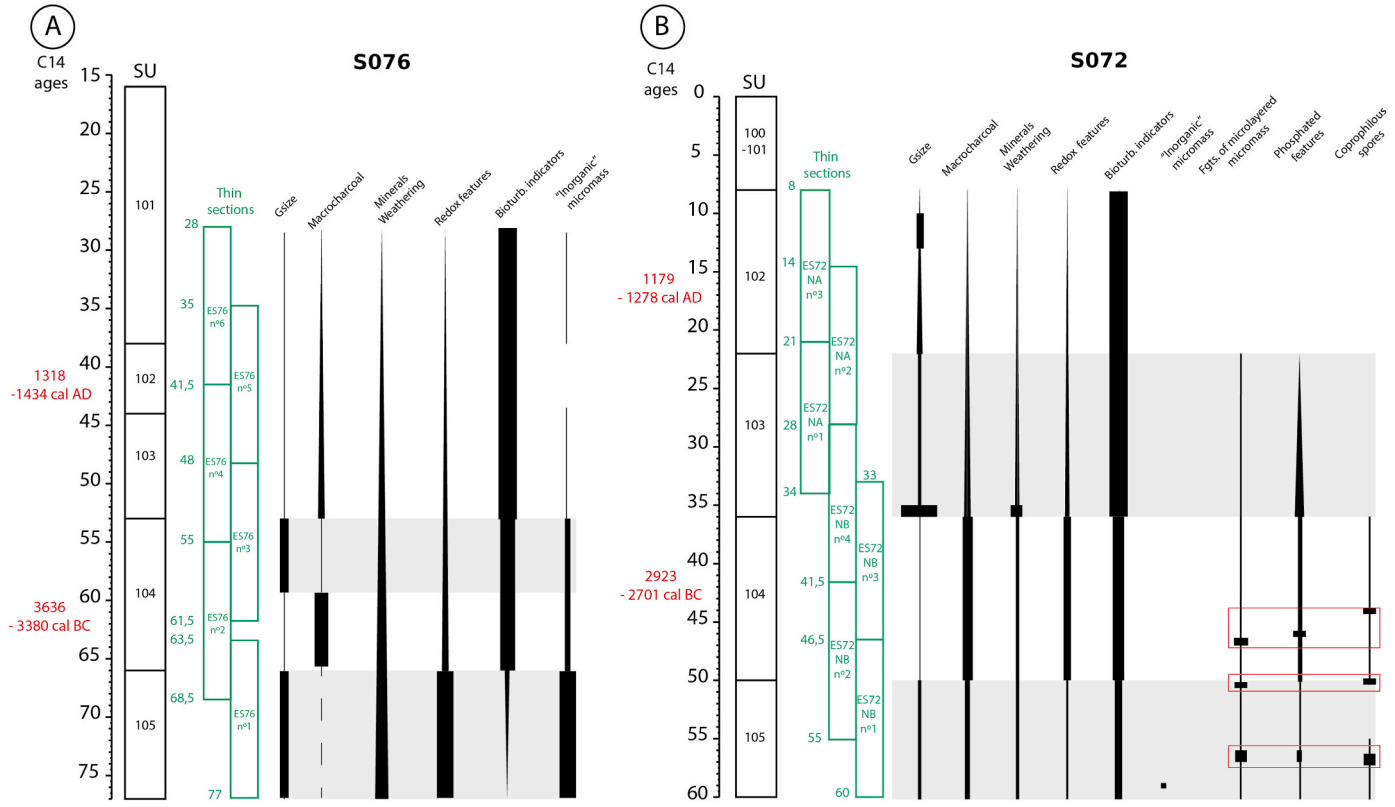

Fig. 5. Summary diagram of selected micromorphological features of S076 (A) and S072 (B). Bar widths indicate relative abundance, or development degree of features. Grey and white backgrounds represent proposed phasing, based on micromorphological evidence. Red rectangles in B mark clusters combining fragments of microlayered micromass, phosphated features and spores of coprophilous fungi. Gsize: Grain-size.

interpreted as an accretion of colluvial material together with highly increased pedological activity and significant enrichment in organic matter in broadly drier conditions. The unit shows a bipartite pattern regarding grain-size and macrocharcoal (Fig. 5): its lower half is finer and rich in large, millimetric macrocharcoals, whereas the upper half lacks macrocharcoal but exhibits a much larger grain-size (up to small gravels and gravel-sized pedosedimentary aggregates), suggesting detrital inputs from soils around. This indicates that intense in situ burning of wood and plant materials, identifiable as a phase of use of the structure, occurred during the deposition of the lower part of the unit and were interrupted by a phase of erosion or degradation of the structure.

Upper units of the infilling (SU76103, 76102, and base of 76101) present rather homogeneous characteristics (see Fig. 5), with a relatively reduced grain-size, limited presence of weathering and redox features, and a moderate amount of macrocharcoal in a globally very bioturbated context. These three SUs are easily interpreted as the gradual infilling and thickening of the structure stratigraphy by relatively fine colluvial materials in drier conditions, accompanied by an intense reworking by pedogenesis and high biological activity. However, phases in the process of infilling or clear indicators of anthropogenic activities can hardly be distinguished in such SUs. Although macrocharcoals are present, indicating local burning throughout SU76103, SU76102 (dated c. 1370 cal. AD) and SU76101, it seems much less intense than at the base of SU76104. The residual presence of aggregates of inorganic micromass in SU76101 and 76103 can be interpreted as inputs from lateral erosion of more mineral soils.

S072. SU72105 presents a pattern similar to SU76105, although less marked. It has a relatively larger grain size, less (although still important) bioturbation, and less macrocharcoals than overlying units (Fig. A2). Redox features and mineral weathering are here less marked, suggesting that S072 could have retained less water at its base than S076. However, SU72105 and, in general, all S072 include three relevant micromorphological features not detected in S076: fragments of microlayered micromass, phosphatized features, and clusters of spores of coprophilous fungi.

The microlayered micromass appears as small sparse fragments (up to 1 mm) of very thin alternations of fine mineral material of the micromass, with compacted vegetal and organic matter fibers and debris, including aligned phytoliths, and sometimes a slightly spongy structure (Fig. 4-I). Although relatively small and sparse, taking into account the strong taphonomic bias due to pedoturbation in the sequence, these fragments can be considered as relicts of microlayered surfaces of fine mud and litter of vegetal materials. These kinds of layers are usually interpreted as resulting from trampling by livestock and are typical of pastoral enclosures (Shahack-Gross, 2017).

Phosphatized features are also present mainly as fragmented coatings and infillings or more or less intense impregnations of the micromass, sometimes locally evolving to almost pure translucent nodules (Fig. 5). These phosphatic masses are cryptocrystalline neoformed masses, orange or brownish yellow in PPL, with partial to total extinction in XPL (isotropic) and light green under BLF, depending of their purity (Fig. 4-C-D-E). Although the granodioritic substratum suggests rather acidic soils, there are phosphatized minerals stable under these conditions, such as Taranakite or Crandallite (Karkanas, 2010). These phosphatized features are certainly not the result of weathering of granodiorite, but can be considered a post-depositional indicator of the presence of excremental material or dissolved bones from animals in this acidic soil (Karkanas and Goldberg, 2018).

Spores of coprophilous fungi appear sparse in the matrix but especially in well-defined clusters of tens of spores. Although different shapes can be detected (round, lemon-shaped, etc.), the more characteristic is the square or bullet-shaped Sporormiella-type (Fig. 4-H). These clusters of spores, when observed in thin sections, can be

interpreted as an in-situ direct indicator of the presence of significant amounts of dung material in the sequence even if excrements themselves cannot be directly detected due to the intense post-depositional pedo- and bioturbation. In addition, excrements of termites, a known supporter of these fungi, can be excluded as such insects are not present in this high-mountain environment.

Interestingly, higher concentrations of remains of microlayered micromass, phosphatized features, and spores of coprophilous fungi form distinct clusters in S072 where both three appear closely related (Fig. 5). These clusters are located in the middle of SU72105 and at its top (and also in SU72104, see below), suggesting increased presence of dung and/or bones and trampling, and then episodes of the presence of animals in the enclosure following its construction.

A similar cluster of higher concentrations of fragments of microlayered micromass, phosphatized features and spores of coprophilous fungi is present in the lower half of SU72104, the first unit of the infilling of the structure and dated in S072 c. 2800 cal. BC (Fig. 5). SU72104 shows a clearly finer grain-size than the underlying unit, with a more closed structure with partly welded aggregates (granules and crumbles in transition to pseudoblocks) and more redox features. This suggests a gradual infilling with finer materials (and then isolation from detrital fluxes from outside the structure), compaction, and increased retaining of moisture. SU72104 also includes more organic debris, especially macrocharcoal (especially small elongated sticks compatible with grasses), indicating intense burning (Fig. 5). Additionally, a slightly more phosphatized micromass points to sustained presence of dung and/or bones. Despite a relatively higher post-depositional pedoturbation, these features are all consistent with anthropogenic activities and presence of livestock in the structure during the deposition of SU72104, but especially in its lower half, in a bipartite pattern similar to S076.

The top of SU72104 and the transition to SU72103 are characterized by a detrital pulse with coarse sands and gravels, which are certainly amongst the coarsest grains in the sequence and could represent the abrupt end of the previous use of the structure (Fig. 5). A slightly coarser grain-size than SU72104 characterizes SU72103 as colluvial inputs continue to infill the structure, significantly less macrocharcoals (but some still very large, up to 3 mm), less weathering and redox phenomena, and severe pedoturbation. Although fragments of layered micromass and phosphatized features are still present, they are much scarcer and do not form clear clusters. This layer continues to reflect regular human activity (persistence of burning) and the presence of animals. However, the signal is somewhat weaker and certainly also more blurred by a strongest pedoturbation. SU72102, dated around 1200 cal. AD, is quite similar to SU72103. However, fragments of microlayered micromass and phosphatized features disappear. In contrast, later detrital pulses continue to infill the structure and thicken the pedological profile

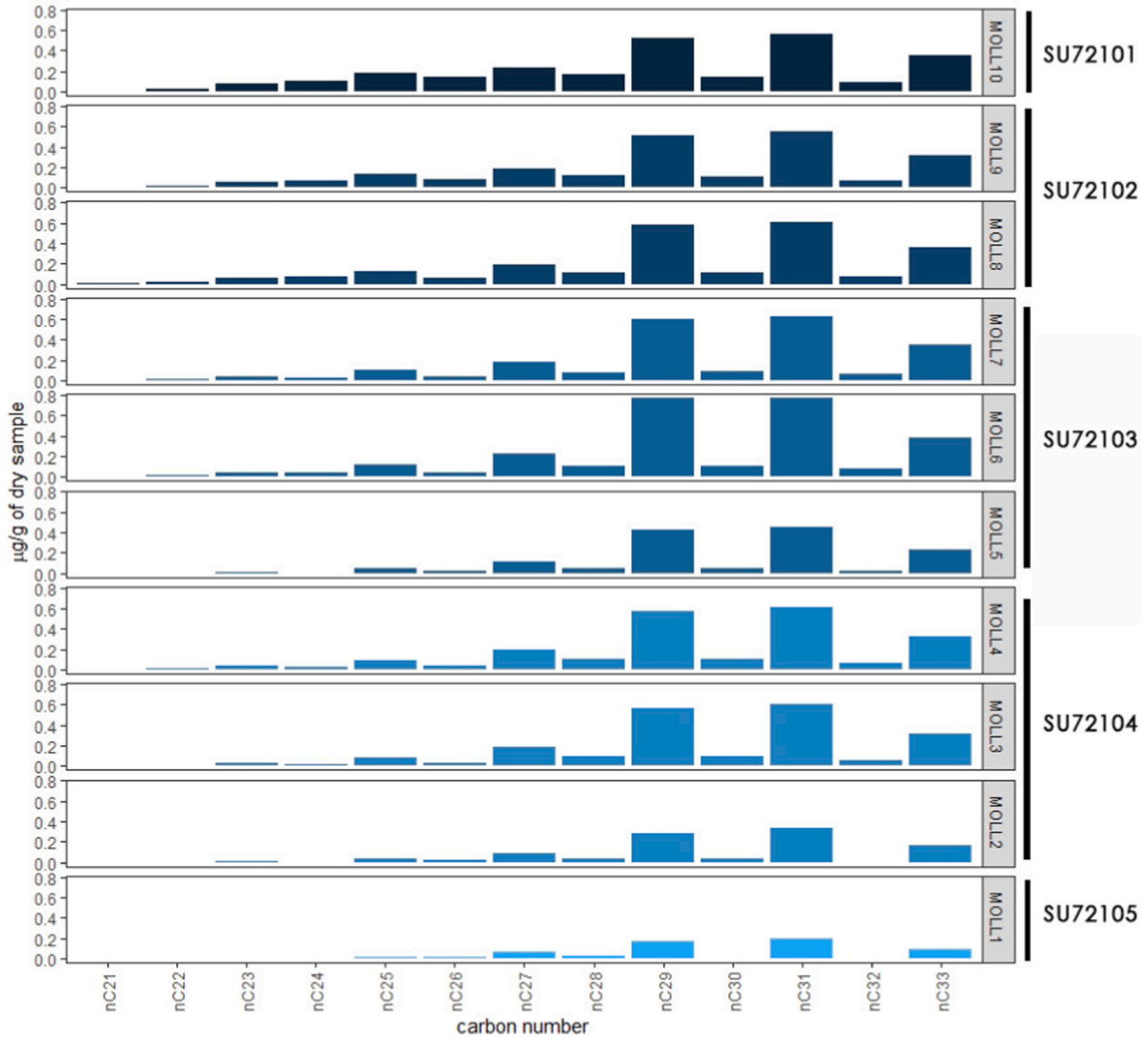

Fig. 6. Barplot showing distribution and abundance of *n*-alkanes for each sample and Stratigraphic Unit. Concentrations are expressed as µg of individual compound per gram of dry sample.

(Fig. 5). It cannot be said if this is due to a taphonomic bias resulting from the increasing pedoturbation to the top of the sequence, or a gradual decay in the frequency and intensity of use of the structure.

4.5. Biomolecular results

4.5.1. n-Alkanes

n-Alkanes originate from epicuticular waxes of vascular higher plants and are chemically inert, non-polar saturated hydrocarbon molecules (Eglinton and Hamilton, 1967). They are usually well preserved in soils and lacustrine sediments and could preserve authentic stable isotope ratios for geological time scales (Cranwell, 1981; Ardenghi et al., 2017). Changes in *n*-alkane ratios in sedimentary records have frequently been interpreted to reflect changes in local vegetation cover. Thus, these properties make *n*-alkanes one of the most reliable biomarkers for palaeoenvironmental reconstruction (Sachse et al., 2006; Niedermeyer et al., 2010, 2016; Schemmel et al., 2016), and past human-environment interactions and human evolution studies (Patalano et al., 2021).

The distribution and abundance of *n*-alkanes for each sample and SU are reported in Fig. 6. Concentrations of *n*-alkanes in the samples varied between 0.00010 and 0.77140 μg/g of dry sample, with the lowest recovered in sample MOLL1 pertaining to SU72105. *n*-Alkanes abundance in soils is highly related to overlying vegetation (Schäfer et al., 2016), and croplands and sparse grasslands cover usually have low reported *n*-alkanes concentrations. In our samples, all plant lipid profiles include –mid and long-chain *n*-alkanes (>nC_{21}) and predominance of odd carbon numbers. All soil samples exhibited maximum abundance at nC_{31}, generally accepted as related to grass cover, although some conifer groups, such as Podocarpaceae and Araucariaceae can also produce large amounts of nC_{31} alkanes (Schlanser et al., 2020). High quantities of nC_{29} alkanes were detected, usually related to shrubby and tree vegetation types. Another abundantly found alkane is nC_{33}, characteristic of grasses, some conifers, the *Juniperus communis* shrub, and other plants from the Cupressaceae family (Carrero-Carralero et al., 2022). Land cover along the sequence seems to generally be that of a grassland with small communities of shrubs and conifer woods. It appears that vegetation inputs into the sedimentary record do not vary much over time, except for samples MOLL6 and MOLL7 (SU72103), where an increment in nC_{29} (shrubs/trees) can be observed. Gymnosperm tree species, for example, *Pinus sylvestris* and, in general, the *Pinaceae* family, produce a very low amount of *n*-alkanes, while angiosperms tend to produce larger amounts (Aichner et al., 2018; Schlanser et al., 2020). Thus, this could indicate that shrubs and patches of trees might have slightly recolonized the space, one possible interpretation being a less intense site occupation at that period.

The carbon preference index (CPI) is used here as a reference indicator for organic matter maturation, preservation, and environmental conditions. CPI values for our nC_{21}~nC_{33} alkanes ranged from 3.10 to 14.79 (Fig. 7), indicating good preservation of immature organic matter originated from terrestrial higher plants. Generally, high values of CPI correlate with cold and dry conditions, while low values (=<1) relate to warmer environments, recycled organic matter, petrogenic input, or/and bacterial activity (Connolly et al., 2019). In our case, there is a slight poorer preservation of these biomolecules where values decrease with depth (older organic matter), but no bacterial activity is detected.

The average chain length (ACL) ranged from 29.67 to 30.02, this small variation reflecting low rates of evapotranspiration and generally stable environmental conditions along the sequence. Moreover, forest vegetation usually yields average shorter chain lengths (lower ACL) than plants from grasslands. Thus, our results indicate a sustained grassland landscape cover with very few variations (Fig. 7).

Paq index values higher than 0.4 would indicate that more contributions are assumed from submerged/floating macrophytes to the total *n*-alkane pool. Paq values < 0.1, only a little contribution from the freshwater body is expected. Values between 0.1 and 0.4, indicate more contributions from emergent macrophytes. Here, samples from SU72101 and SU72102 seem to have small contributions of emergent macrophytes. In contrast, the rest of the SUs have more terrestrial input (woody shrubs and grasses) (Fig. 7). Common examples in the Pyrenees lake catchments, ponds, peats, bogs, swamps, and wet grasslands are *Ranunculus flammula* and *Juncus squarrosus*, both perennial herbaceous that are currently present in the site surrounding local vegetation.

4.5.2. Compound-specific carbon and deuterium isotope analysis

The most common stable isotope used as an environmental and dietary indicator is $\delta^{13}C$ (ratio between carbon-13 and carbon-12). This is partly due to its effectiveness as an environmental proxy, which enables us to trace plant type, plant water-use efficiency, and relative paleotemperature based on the distinct ratio between the ^{13}C and ^{12}C isotopes found within leaf lipid compounds. Leaf wax lipid $\delta^{13}C$ values of *n*-alkanes have been shown to vary between −29‰ and −39‰ in C3 plants and between −14‰ and −26‰ in C4 vegetation.

Leaf wax *n*-alkanes stable hydrogen isotope composition (δD) contains ecohydrological information that can be preserved over millions of years. δD values reflect both the δD values of precipitation, deuterium-enriched leaf water, and evapotranspiration (Kahmen et al., 2011). Monocotyledonous (grasses) are deuterium depleted relative to dicotyledonous (forbs, shrubs, trees) species, and in general, more negative values indicate wetter conditions, and more positive values indicate drier conditions (Liu et al., 2016). Present-day $\delta^{2}H$ (‰, V-SMOW) are estimates according to *The Online Isotopes in Precipitation Calculator, version 3.1* (Bowen, 2022).

Our nC_{29} and nC_{31} $\delta^{13}C$ samples values vary between ca. −31.4‰ and −32.6‰ (mean 32‰), indicating the presence of C3 plants all along the sequence, with the sequence cooler conditions observed in SU72104 corresponding to the Late Neolithic (2923 - 2701 cal. BC).

δD values for the same *n*-alkane $C_{numbers}$ are between −212.8‰ and −228.9‰ (mean −218.1‰). The lowest value of nC_{29} −223.7‰ and nC_{31} −228.9‰, are recorded in sediments of SU72104, indicating more

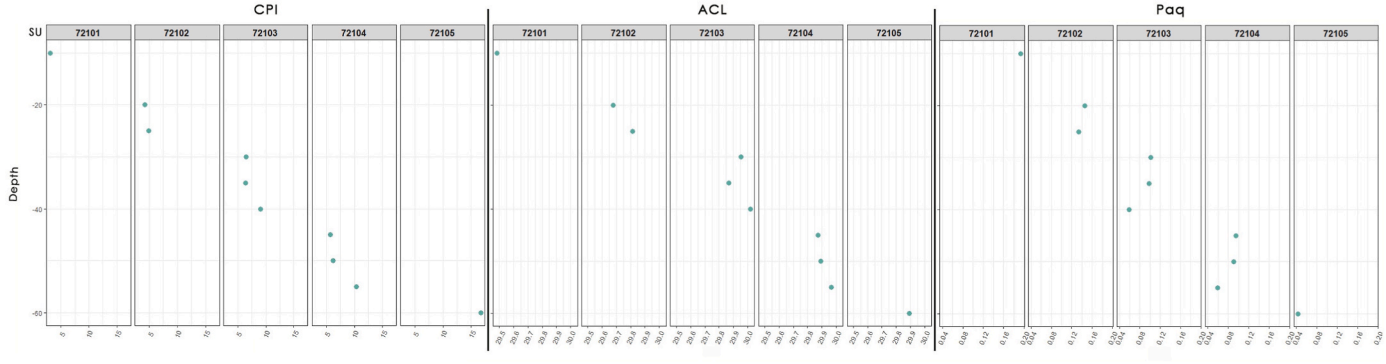

Fig. 7. CPI, ACL and Paq index results for each sample and Stratigraphic Unit.

humid conditions. This phase is followed by a drier period observed in SU72103, with values for nC_{29} −213.3‰ and nC_{31} −214.6‰ (Fig. 8).

4.5.3. Polycyclic aromatic hidrocarbons and alchols

Polycyclic aromatic hydrocarbons (PAHs) are a class of chemicals that occur naturally in coal, crude oil, and gasoline. They also are produced when coal, wood, food, and garbage are burned. PAHs generated from these sources can bind to or form small particles in the air and are trapped in sediments.

All analyzed samples in Molleres II have the presence of retene. The presence of traces of retene in the air and sediments is an indicator of forest fires and pollution, and it is a major product of the pyrolysis of conifer trees. Moreover, this compound occurs naturally in the tars obtained by the distillation of resinous woods, derived by the degradation of specific diterpenoids biologically produced by conifer trees. No diterpenoids or triterpenoids from conifer species were detected in any of the samples. Specifically, chromatograms with characteristic ion fragments *m/z* were extracted for abietic acid (TMS) (259, 287, 302), dehydroabietic acid (TMS) (239, 357, 372), and 7-oxodehydroabietic acid (TMS) (253, 268, 386) with no positive results. Conifers store large amounts of terpenoids in resin ducts of various tissues (Duan et al., 2020). When high temperatures are produced, degradation of these diterpenoids starts, following a product-precursor diagenetic path from dehydrogenation of abietic acid to dehydroabietic acid, decarboxylation to dehydroabietin, and then full aromatization to retene (Medeiros and Simoneit, 2007). Thus, the presence of retene but not terpenes indicates that a high-temperature fire occurred, and terpenes were transformed into aromatic fractions.

4.5.4. Faecal biomarkers: sterols, stanols, and bile acids

Faecal biomarkers, such as sterols, stanols, and bile acids in archaeological studies, are of great interest as they provide insights into both presence of domesticates and past agricultural practices (Evershed et al., 1997; Bull et al., 2002; Prost et al., 2017; Harrault et al., 2019).

In the Molleres II site, we have observed faecal matter remains in all the analyzed sediments along the SU72 sequence, with major steroid compounds such as coprostanol, epi-coprostanol, 5α-stigmastanol, 5β-stigmastanol, and epi-5β-stigmastanol detected (Fig. 9). The total amount of analytes ranges from 0,06 μg/g per dry sediment (MOLL10 SU72101) to 1,71 μg/g per dry sediment (MOLL4 SU72104) (Fig. 9), the latter appearing to indicate more amount of animal dung within the structure when compared to the rest of layers.

The results of the different faecal biomarkers ratios show a positive indication of herbivore ruminant faecal matter in all samples, except for sample MOLL4 (SU72104), which is plotting in the threshold of ratio 1 (Fig. 10). Again, all samples except MOLL4 indicate the presence of herbivore excrement based on Ratio 2. Interestingly, in Ratio 3 all samples point to a ruminant producer. To further investigate sample MOLL4 results, we applied Ratio 4 and 5 to possibly discern if a mixed signal of faecal sources is being detected. Ratio 4, used to distinguish human from ruminant excrement, shows values for all samples below 1.5, indicating no human input, although sample MOLL4 is the only one above 1, the rest being between 0.17 and 0.34. Evershed and Bethell (1996) pointed out that the actual ratio in human faeces is around 5.5 and 0.25 in ruminant faeces, so the likeliness of human or omnivore input is possible. Ratio 5 helped to discern relative human (>73%), and herbivore (<38%) inputs, with values showing a definitive faecal mixed signal for sample MOLL4 (value of 53.3%) (Fig. 10). Calculation of the derived herbivore input for this sample resulted in 57.2% of herbivore and 42,8% of human/omnivore input.

Bile acids such as Lithocolic acid (LCA) and Deoxycholic acid (DCA) were detected but with concentrations below the limit of quantification. No other bile acids such as Chenodeoxycholic acid (CDCA), hyodeoxycholic acid (HDCA), or ursodeoxycholic (UDCA) were identified, thus tentatively ruling out a dung origin from human, pig, horse, goat, or goose (Prost et al., 2017). The presence of only LCA and DCA would indicate donkey, cattle, or sheep as the dung matter producer for all samples; although caution should be taken, as the concentration recovery was low. Particular attention should be given to sample MOLL4, where the input of human/pig and ruminant herbivore seems very plausible.

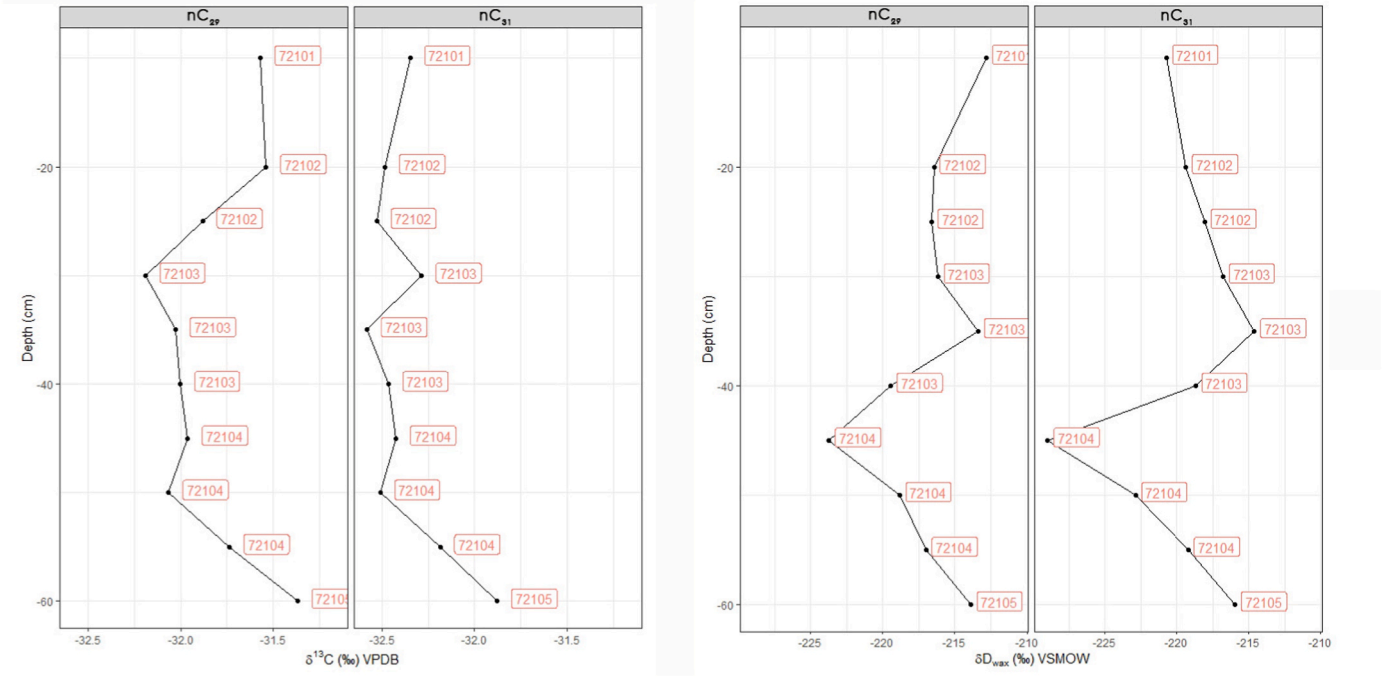

Fig. 8. From left to right: δ^2H_{wax} for *n*-alkanes C_{29} and C_{31}, and $\delta^{13}C_{wax}$ for *n*-alkanes C_{29} and C_{31}, in relation to depth.

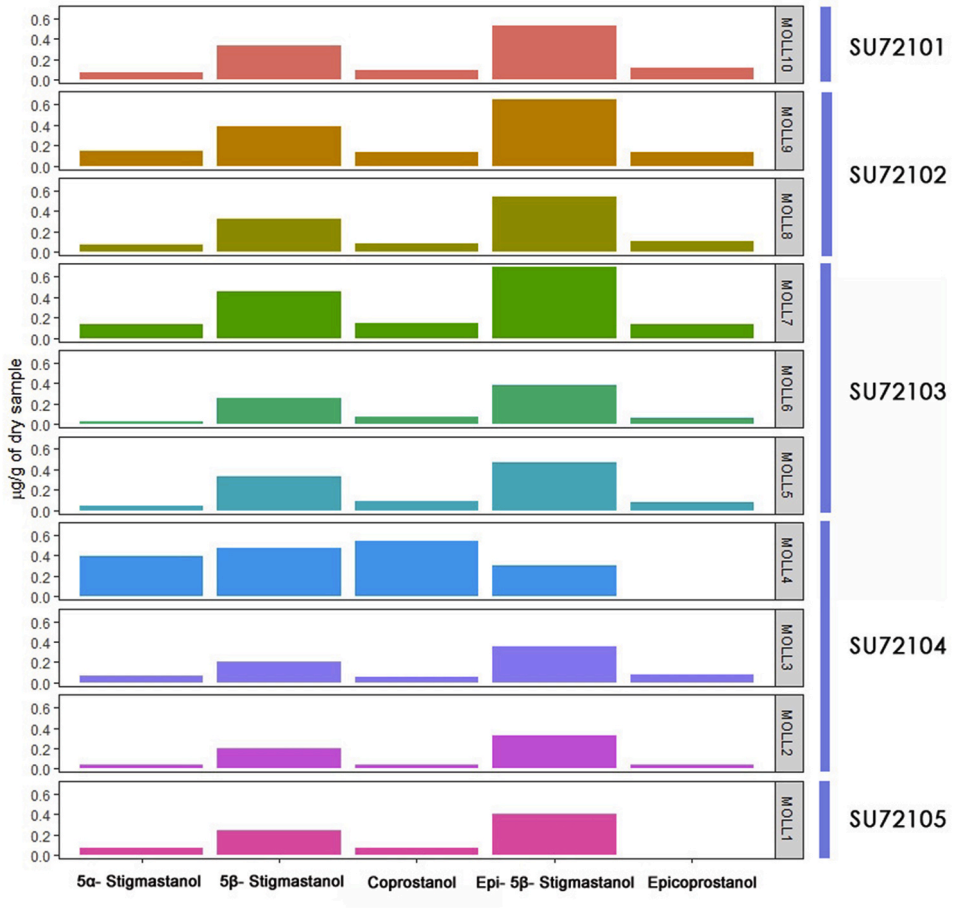

Fig. 9. 5β-stanols, and cholesterol-derived 5β-stanols (coprostanol and epicoprostanol) concentration for each sample and Stratigraphic Unit. Concentrations are expressed as µg of individual compound per gram of dry sample.

5. Discussion

5.1. Molleres II: a fenced space from the Neolithic to the Middle Ages

Taphonomic and post depositional processes are especially intense in high mountains preventing a complete understanding of archaeological contexts located in these areas due to the degradation of the scarce evidence, and Molleres II site is not an exception. A very intense and constant pedo- and bioturbation was observed in the pedosedimentary sequences of the analyzed archaeological structures. Indeed, small earthworms and other microfauna have been detected in the stratigraphy as well as very abundant rootlets forming a thick mat all along the profiles. In turn, this led to a partial blurring of the stratigraphy of the sequence, causing a certain homogenization in terms of color, texture, and structure inside each of the main SUs that were already difficult to distinguish due to the homogeneity of the source material across time. However, Stratigraphic Units were preserved as coherent layers at macro and microscopic levels, as shown by the litho-stratigraphic descriptions and the vertical distribution of key micromorphological features (grain size, organic matter, charcoal, etc.). The limited thickness of the active soil layer (5–10 cm) suggests that churning had a relatively reduced vertical range: then, the greater thickness of the SUs and their cumulic nature explains that their features were slightly blurred but not totally homogenized. The same applies to the analyzed lipid biomarkers, which are predominantly adhered to the fine fraction of the sediment and are constituents of the organic matter. Although a limited vertical migration or mixing of these two soil components cannot be discarded, litho-stratigraphic and micromorphological data show that they have a clear stratigraphic distribution and are not significantly affected by post-depositional translocation. Moreover, the discontinuous signal of most biomarkers across the profiles, showing several peak distribution patterns instead of vertically homogeneous or top-down decreasing distribution, also suggests that a potential postdepositional migration from above was certainly limited and that the signal can be safely interpreted assuming the relatively low-resolution and certain background noise.

The shape and size of the structures, the constructive characteristics of the stone walls, and the stratigraphic sequence observed during the excavation, together with its soil micromorphology have made it possible to interpret the site of Molleres II as a space with fences of about 744 square meters made up of 5 different structures.

The excavated structures generally show a stratigraphic sequence similar to each other, especially at their base. Layers characterized by “inorganic” micromass and very limited soil activity or disturbance are present in the deepest analyzed test pits (i.e., SU72105, SU73105, and SU76105). They represent the palaeosoil on which the perimeter walls of the enclosures (SU72120, SU73120, and SU76120) were set. The construction of these enclosures favored the retention of the fine colluvium from upslope soil, causing a significant soil thickening. Structures 072 and 076 clearly show this steady accumulation of colluvium derived from neighboring soils and granodioritic regolith combined with its gradual and constant pedogenesis, leading to a terrace-shaped profile of the structures. This gradual infilling was accompanied by a marked enrichment in organic matter and charcoal remains, but also by enhanced soil biological and pedogenic activity allowed by the thickening of the profile, and led to the development of a thick A organo-mineral horizon (umbric leptosol).

Unlike the underlying deposit, the first filling layers of the enclosures (SU72104, SU73104, and SU76104) clearly show this increase of

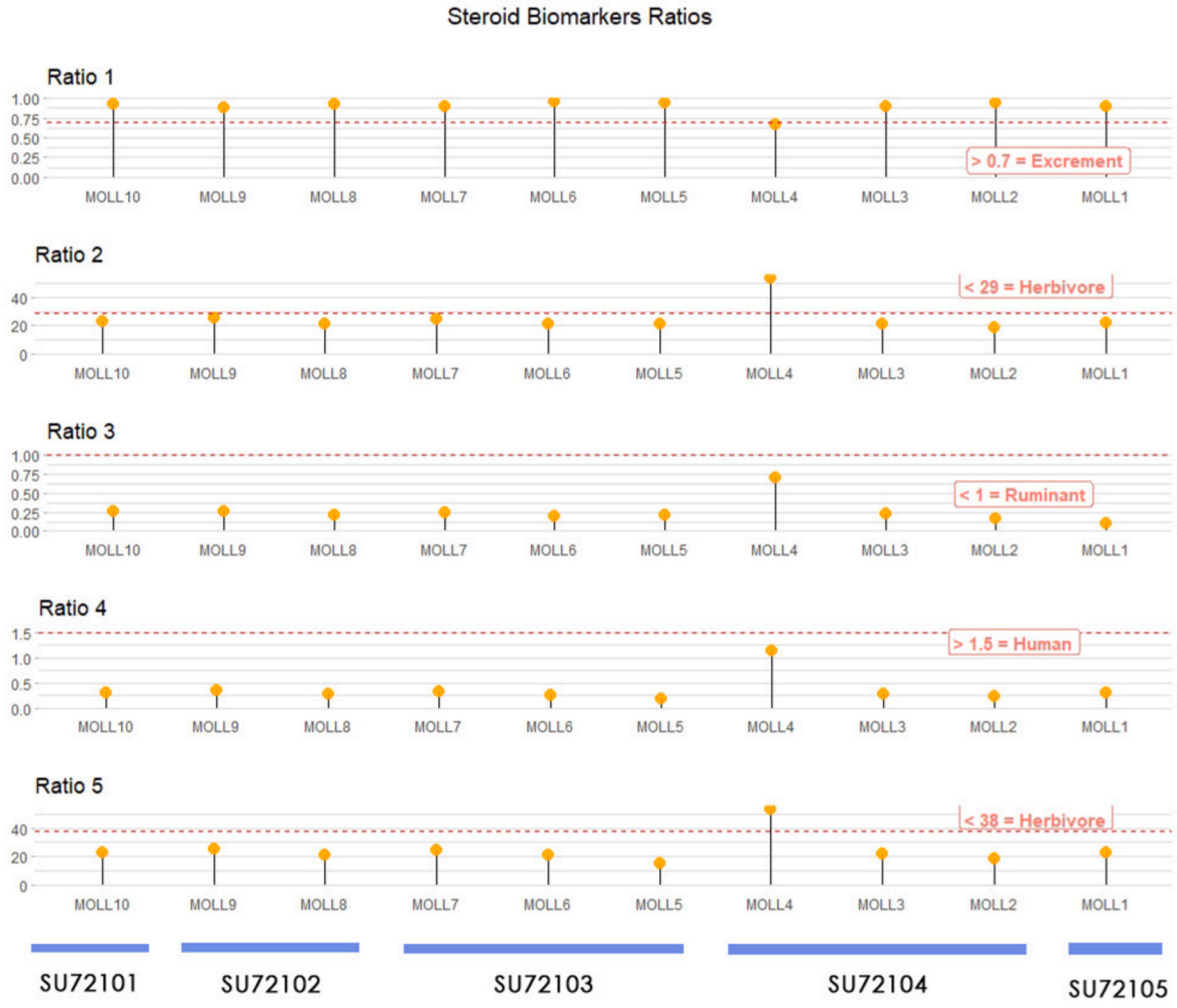

Fig. 10. Faecal steroids ratios (see section 3.4,) with values calculated for each sample in relation to each Stratigraphic Unit.

organic matter (including the presence of faecal matter in the case of S072), macrocharcoals and soil activity/disturbance; in high mountain contexts (where archaeological material is rarely preserved) these features are commonly associated with anthropogenic activities thus corresponding with occupation and use of the structures (Orengo et al. 2014a, 2014b). The radiocarbon dating obtained in all three occupational layers shows a chronology corresponding to the Middle/Late Neolithic. Specifically, SU76104 is dated to the end of the Middle Neolithic (Poz-133848: 3636 – 3380 cal. BC) and the transition to the Late Neolithic, thus making Molleres II the older extensive enclosures, delimited by large dry stone walls, known in this sector of the Eastern Pyrenees. Investigations conducted by Rendu (2003) in the Enveig mountain (French Cerdagne) as well as by GIAP researchers in Madriu and Perafita valleys (Andorra) (Ejarque, 2013; Orengo et al., 2013) attested to the increase of livestock activities in this period, but in no case, such extensive and complex livestock site had been documented.

The deposit accumulated after the Neolithic occupation until nowadays is quite homogeneous as highlighted by both stratigraphical and micromorphological observations: layers with marked anthropogenic signals characteristic of the Neolithic phase are more difficult to identify here. Nevertheless, there are some discontinuities in terms of organic matter amount, macro- and microcharcoals presence, and archaeological remains (e.g., pottery) that might be interpreted as phases of greater or lesser intensity of use of the fences.

Following the Neolithic phase there was a probable period of abandonment or less intense use (SU72103, SU73103, and SU76103) marked by increased detrital influxes in drier conditions and a reduction of macrocharcoals presence. A slight increase in macrocharcoals and organic matter was most clearly evidenced in the SU72102 and SU76102, probably associated with a second phase of enclosures occupation. The discovery of pottery in these layers (SU73102 and SU76102) strengthens this hypothesis. Radiocarbon dating obtained from SU102 in both S072 and S076 fits each other showing a chronology related to the Middle Ages (Poz-130278: 1179–1278 cal. AD; Poz-130427: 1318–1434 cal. AD). Probably connected to this phase (as it overlies the construction of the enclosures) is S075, interpreted as a hut given its shape and small size. This hut was constructed after the enclosures because the enclosures support the walls of the hut; however, previous phases cannot be excluded until pit tests are performed below the collapse layer.

Finally, in the most superficial deposit, no clear signs of another occupation have been detected; indeed, the anthropogenic signals are scarce.

5.2. *Animal husbandry: an in-depth look*

Archaeological and chrono-stratigraphic evidence shows that Molleres II is a space with 4 different fences and a possible hut establishing a long chronology of use that started from the end of the Middle Neolithic with a likely second phase of more intense occupation during the Middle Ages. By studying specific micromorphological features and biomolecular markers, it was possible to identify the function of these enclosed spaces.

The occurrence of trampling evidence (i.e., presence of remains of microlayered surfaces) and high amount of animal dung (i.e.,

occurrence of phosphatic features, faecal biomarkers, and spores of coprophilous fungi) hint at a pastoral use of the fences. This is particularly evident in S072, where a cluster of these features has been detected in the middle/top of SU72105 and the base of SU72104. This suggests the increased presence of dung and/or bones and trampling, and then episodes of the presence of animals in the enclosure following its construction. The existence of this cluster in the central and upper part of SU72105 (the original soil profile) should not be surprising: the disturbing activity (e.g., trampling or scratching by livestock or just pedoturbation processes) produced in the overlying layer (SU72104) could have easily introduced these features a few cm below. In addition, favorable taphonomic conditions such as reduced redox fluctuations and cooler and drier conditions could then have helped to the preservation of these features at this depth. The decrease of faecal biomarkers at the top of SU72104 might also suggest the beginning of a phase of abandonment of the structure or lower animal pressure. This lower pressure also seems well evidenced by the decrease and ultimately disappearance of trampling evidence and coprophilous fungi in the subsequent layers of S072 (SU72103 and SU72102). It has to be noted that faecal biomarkers remain constant along the profile suggesting a regular (albeit seasonal) occurrence of animals in this space. Although the taphonomic issue cannot be totally excluded among the processes that generated these discontinuities in the micromorphological record, the regular but less intense animal presence in this space fits with the archaeological evidence (see paragraph 5.1), showing a decrease in anthropogenic pressure after the Neolithic period but not its complete disappearance. Not surprisingly, during the archaeological survey, others structures were identified in the Puigpedrós-Malniu mountain range, with chronologies from Bronze Age onwards (Colominas et al., in press). Although investigations for these sites are still ongoing, it is possible that they played a role in the management of livestock in these highlands.

Although micromorphological and biomolecular investigations were not carried out in S073 and S074, the similarity with S072 (in terms of stratigraphic sequence and its macroscopic characteristics) suggests a similar function of these fences.

Therefore, Molleres II could be interpreted as a livestock space built in the Middle/Late Neolithic for pastoral purposes (housing of animals), subsequently subject to the same use, although with periods of greater or lesser intensity.

Faecal biomarkers also allowed us to better define the animal species stabled in these enclosures. Sterols and stanols from all along the stratigraphic profile of S072 indicate the presence of ruminant herbivores, goats and horses excluded, and possible human/omnivore input during the Late Neolithic (documented in just one sample); bile acids are indicative of sheep/cattle origin although as stated before, the recovery was low, and caution should be taken. However, this evidence is of crucial importance as archaeozoology cannot always determine which animal species were exploited in high mountain spaces (Colominas et al., 2020). Uplands are indeed affected by strong erosional and frost/thaw processes, and sometimes, the high acidity of the soils prevents the correct conservation of animal bones.

Therefore, through this multi-proxy approach, we suggest that these structures were contemporary enclosures and that they were used to predominantly stable sheep and/or cattle. These two species are present in all the Middle and Late Neolithic sites from the Pyrenees, where faunal remains have been recovered. They have been documented at Coro Trasito cave (Sobrarbe, Huesca, 1548 a.s.l.) (Gassiot et al., 2020); at Els Trocs cave (San Feliú de Veri, Huesca, 1564 a.s.l.) (Rojo Guerra et al., 2013); at Cova del Sardo cave (Boí, Lleida, 1790 a.s.l.) (Gassiot et al., 2015); and at Puyascada cave (Espluga de la Puyascada, Huesca, 1320 a.s.l.) (Castaños, 1984). Domestic animals constitute the main component of all faunal assemblages recovered at these sites. Among domesticates, sheep are the most documented species, although cattle, goats, and pigs are also attested.

The study of sheep/goat kill-off patterns from Coro Trasito shows that these species were slaughtered at younger ages for their meat but probably also to obtain milk (Gassiot et al., 2020). A similar pattern has been documented at Els Trocs, in which sheep/goat slaughtering patterns suggest a husbandry strategy oriented to tender meat production with marginal exploitation of milk (Tejedor-Rodríguez et al., 2020). Therefore, our data aligns well with the archaeozoological data recovered from Pyrenean sites around 1000–2000 m a.s.l. The enclosures of Molleres II, however, are located at 2425m a.s.l. We do not intend to resolve here the debate about the existence of specialized pastoralism that could involve seasonal movements during the Neolithic (see, for example, Rojo Guerra et al., 2013; Rojo Guerra et al., 2014; Tornero et al., 2016; Antolín et al., 2017; Tejedor-Rodríguez et al., 2020) but the data presented here demonstrate the presence of large enclosures for sheep and/or cattle in an area only seasonally available, showing the arrival of an important number of sheep and/or cattle to exploit summer pastures.

5.3. Environmental dynamics and fire use

Anthracological, micromorphological, and biomolecular data have provided valuable clues for identifying local (site scale) environmental characteristics and their changes over time. However, they need to be handled with care as they are subject to bias related to the limited representativeness of the locally observed evidence, making their extrapolation complex at a broader landscape-scale. Additionally, they depend on both the context and history of use of the structures and are also partly hampered by taphonomic issues. Despite these limits, cross-checking the different proxies allowed us to interpret some relevant elements of the environment characterizing the site and its immediate surroundings.

The analysis of the first layer at the base of the test pits profiles (i.e., SU72015, SU73105 and SU76105) has shed light on the main features of the thin palaeosoil preceding the onset of anthropic activities. It is characterized by a very mineral micromass, a reduced amount of phytoliths, limited bioturbation, and very few charcoal fragments. Therefore, site environmental conditions would be characterized by a leptosol on granodiorites, scarcely covered by herbaceous and shrubby vegetation, likely similar to those present nowadays around the structures. This hypothesis is reinforced by the observed *n*-alkanes composition, linked to common woody and herbs cover, with δD values associated with drier present-day conditions. The presence of some pine charcoal remains (i.e., SU73105) could be due to the presence of sparse individuals of mountain pine, which easily grow in rocky areas with twisted or bushy shapes, albeit they could also have been injected from overlying layers due to pedoturbation (see paragraph 5.2).

In such layers, corresponding to the construction and occupation phase of the enclosures during the Middle/Late Neolithic, the site environmental conditions changed. A clear increase in phytoliths content and the *n*-alkanes ratio, together with the presence of charred herbaceous plants, suggests a locally more developed grass cover (see also higher ACL), even if the occurrence of mountain pine remains also hints at the presence of arboreal and/or shrub vegetation. Although anthracological interpretation is hampered by the impossibility of establishing the origin of the charcoal fragments in our high-mountain pastoral enclosures, integration with multi-proxy data allows formulation of some hypotheses for the Molleres II site. An external origin of charcoal remains is unlikely due to the presence of the retene among the polycyclic aromatic hydrocarbons, indicating locally burnt conifers. The size of the charcoal fragments and their “fragile” shapes in micromorphological thin sections also indicate an *in situ* combustion and tend to discard any transport. Thus, charcoal presence could be correlated with the constructive characteristics of the enclosures or to the pastoral practices that were carried out in them. On the one hand, charcoal remains may have originated from the burning of the structures; however, no evidence of palisades was found (e.g., post holes) during the excavation, and fences were built exclusively with stone walls. As the presence of a roof covering (even partially) the structures cannot be

excluded, charcoal could have instead been derived from the combustion of this building element.

On the other hand, fire inside animal fences might be linked to specific pastoral practices.

Ethnographic and archaeological research have demonstrated that sanitation practices of the stables commonly involve a recurrent use of fire, especially in the case of caves and closed (roofed) structures (Gabellieri et al., 2020). It is common to build fireplaces in very cold environments to warm the animals, particularly at night. However, in this case, the distribution of the charcoal fragments should have been more concentrated (as in the cases of domestic hearths), while in the analyzed layers the charcoal remains are rather dispersed, although this could be due to trampling and other pedoturbation processes. Furthermore, the likely presence of pine leaf (needle) and herbaceous species among the charred material may suggest their use as the roof covering or as animal litter.

The anthracological data collected at Molleres II fits with a well-documented framework of widespread use of mountain pine during the Middle/Late Neolithic (e.g., Orengo et al., 2014a; Ejarque, 2013; Gassiot et al., 2012; Rendu, 2003; Euba and Palet, 2010; Gómez et al., 2021; Galop, 2014) often related with pastoral practices.

The occurrence of phytoliths, charcoal fragments, and *n*-alkanes in the subsequent layers is evident and quite constant along the whole stratigraphic profile, indicating the sustained presence of grasslands/shrublands and burning (probably related to pastoral activities) in later phases.

It has to be noted that despite the wide use of mountain pine during the Neolithic onwards, it remains present in later periods, suggesting that the threshold of (local) overexploitation and the subsequent scarcity of this resource was never reached. All this evidence can indicate the long-term stability of a local alpine grassland landscape with scattered mountain pines populations since the onset of the Neolithic pastoral use.

Shrubs' recolonization phases suggested by *n*-alkanes variations (SU72103) could be linked to a possible abandonment or less intensive use of this space (see paragraphs 5.1 and 5.2). This potential hiatus is also supported by the scarcity of fire and animal presence markers (macro- and microcharcoals, layered micromass and phosphatized features although taphonomic biases may exist) and a marked detrital pulse, with coarser sands and gravel arriving into the structure.

6. Conclusion

The investigations at Molleres II offered further insight into the occupation dynamics of high mountain spaces in the Eastern Pyrenees. Despite the strong post-depositional processes affecting the taphonomy of the archaeological stratigraphy, the multi-proxy analysis applied in this study allowed to characterize the site and the chronology of the different occupation phases, to reconstruct the life history and possible use of the structures, and to outline the main environmental dynamics in their surroundings.

By the end of the Middle Neolithic (middle of the 4th mil. cal. BC) four enclosures were built and likely used during some centuries (beginning of the 3rd mil. cal. BC) for sheep and/or cattle housing: Molleres II was set up as a complex and wide open-air site, located exceptionally high and dedicated to the seasonal animal husbandry. These unique settings make the site a primer for this period and in the Eastern Pyrenees, where Neolithic occupational sites tend to be located in caves or shelters. Our results also highlight the intensity of the animal presence since the Prehistory in these uplands, which turns out to have been considerable.

Later phases are more difficult to interpret even though the animals' presence, although weaker, still seems persistent and shows a renewed intensity during the Middle Ages.

This intense and long-term animal presence in the Pyrenean highlands since the Neolithic could be at the origin of stable grassland-dominated environments and open landscapes maintained (albeit with some discontinuities) until nowadays. Further research challenges will be focused on expanding the local glimpse provided by this study and providing a more profound and landscape-scale understanding of the environmental transformations caused by the first pastoral societies in the eastern Pyrenees.

Author contributions

V. Pescini: Conceptualization, Investigation (archaeology and anthracology), Writing – Original draft, Editing & Review. **A. Carbonell:** Conceptualization, Investigation (archaeology, GIS), Writing – Original draft, Editing. **L. Colominas**: Conceptualization, Investigation (archaeology), Writing – Original draft, Editing, Funding acquisition. **N. Égüez**: Conceptualization, Investigation (biomolecular analysis), Writing – Original draft, Editing. **A. Mayoral**: Conceptualization, Investigation (soil micromorphology), Writing – Original draft, Editing. **J.M. Palet**: Conceptualization, Investigation (archaeology, remote sensing prospection), Writing – Original draft, Editing, Funding acquisition.

Data availability

Other data than those included in the text can be obtained on request from the authors.

Funding

This study is part of the larger multi-scale and interdisciplinary projects "TransLands" and "TranScapes", funded by the Spanish Ministry of Science (PGC2018-093734-B-I00 & PID2021-127064NB-I00) and the Catalan Goverment (CLT009/18/00101 & CLT009/22/00035), and developed in the Pyrenean Axial mountain range in La Cerdanya. Lídia Colominas is funded by a Ramón Cajal contract (RYC2019-026732-I-AEI/10.13039/ 501100011033). Valentina Pescini is funded by a Ramon Cajal - junior contract (RYC2021-034621-I – "Transeant" Project). Alfredo Mayoral is funded by a Juan de la Cierva-Incorporación contract (IJC2020-045609-I). Natalia Égüez is funded by a Marie Skłodowska-Curie Actions Individual Fellowship (IBERHUNT-101032608).

Declaration of competing interest

The authors declare that they have no known competing financial interests or personal relationships that could have appeared to influence the work reported in this paper.

Acknowledgment

NE would like to thank AMBI-Lab members H. Padrón-Herrera and A.V. Herrera-Herrera for their help with the saponification extraction method.

Appendix A. Supplementary data

Supplementary data to this article can be found online at https://doi.org/10.1016/j.quaint.2023.04.008.

References

Aichner, B., Ott, F., Slowinski, M., Norygkiewicz, A.M., Brauer, A., Sachse, D., 2018. Leaf wax *n*-alkane distributions record ecological changes during the Younger Dryas at Trzechowskie paleolake (Northern Poland) without temporal delay. Clim. Past 14 (11).

Allué, E., Martínez-Moreno, J., Royc, M., Benito-Calvo, A., Mora, R., 2018. Montane pine forests in NE Iberia during MIS 3 and MIS 2. A study based on new anthracological evidence from Cova gran (Santa Linya, Iberian pre-Pyrenees). Rev. Palaeobot. Palynol. 258, 62–72. https://doi.org/10.1016/j.revpalbo.2018.06.012.

Antolín, F., Navarrete, V., Saña, M., Viñerta, A., Gassiot, E., 2017. Herders in the mountains and farmers in the plains? A comparative evaluation of the

archaeobiological record from Neolithic sites in the eastern Iberian Pyrenees and the southern lower lands. Quat. Int. 484 (810), 75–93.
Ardenghi, N., Mulch, A., Pross, J., Niedermeyer, E.M., 2017. Leaf wax *n*-alkane extraction: an optimised procedure. Org. Geochem. 113, 283–292.
Asouti, E., Austin, P., 2005. Reconstructing woodland vegetation and its exploitation by past societies, based on the analysis and interpretation of archaeological wood charcoal macro-remains. Environ. Archaeol. 10, 1–18.
Bowen, G.J., 2022. The Online Isotopes in Precipitation Calculator version X.X. http://www.waterisotopes.org.
Bray, E.E., Evans, E., 1961. Distribution of n-paraffins as a clue to recognition of source beds Geochem. Cosmochim. Acta 22, 2–15.
Bronk Ramsey, C., 2020. The IntCal20 Northern Hemisphere radiocarbon age calibration curve (0–55 cal kBP). Radiocarbon 62 (4), 725–757.
Bull, I.D., Lockheart, M.J., Elhmmali, M.M., Roberts, D.J., Evershed, R.P., 2002. The origin of faeces by means of biomarker detection. Environ. Int. 27 (8), 647–654.
Bullock, P., Fedoroff, N., Jongerius, A., Stoops, G., Tursina, T., Babel, U., 1985. Handbook for Soil Thin Section Description. WAINE Research publications.
Bush, R.T., McInerney, F.A., 2015. Influence of temperature and C4 abundance on *n*-alkane chain length distributions across the central USA. Org. Geochem. 79, 65–73.
Carrero-Carralero, C., Ruiz-Matute, A.I., Sanz, J., et al., 2022. From plant to soil: quantitative changes in pine and juniper extractive compounds at different transformation stages. Plant Soil 481, 229–251.
Castaños, P., 1984. Estudio de los restos óseos de la Cueva de Espluga de la Puyascada (Huesca), vol. 4. Revista de arqueología del Instituto de Estudios Altoaragoneses, pp. 43–56.
Chabal, L., 1997. Forêts et sociétés en Languedoc (Néolithique final, Antiquité tardive): l'anthracologie, méthode et paléoécologie. Éditions de la Maison de Sciences de l'Homme, Paris.
Colominas, L., Carbonell, A., Gallego-Valle, A., Martínez, J., Pescini, V., Mayoral, A., Palet, J.-M., 2023. Recerca en espais altimontans ceretans: intervencions arqueològiques a la capçalera del Duran, Vall de la Llosa i sector de Puigpedrós-Malniu (la Cerdanya). Campanyes 2020-2021. XVI Jornades d'Arqueologia de les comarques de Girona.
Colominas, L., Palet, J.M., Garcia-Molsosa, A., 2020. What happened in the highlands? Characterising Pyrenean livestock practices during the transition from the Iron Age to the Roman period. Archaeological and Anthropological Sciences 12 (3). https://doi.org/10.1007/s12520-020-01023-3.
Connolly, R., Jambrina-Enríquez, M., Herrera-Herrera, A.V., Vidal-Matutano, P., Fagoaga, A., Marquina-Blasco, R., Marin-Monfort, M.D., Ruiz-Sánchez, F.J., Laplana, C., Bailon, S., Pérez, L., Leierer, L., Hernández, C.M., Galván, B., Mallol, C., 2019. A multiproxy record of palaeoenvironmental conditions at the Middle Palaeolithic site of Abric del Pastor (Eastern Iberia). Quat. Sci. Rev. 225, 106023.
Courty, M.A., Allué, E., Henry, A., 2020. Forming mechanisms of vitrified charcoals in archaeological firing assemblages. J. Archaeol. Sci. https://doi.org/10.1016/j.jasrep.2020.102215. Report 30.
Cranwell, P.A., 1981. Diagenesis of free and bound lipids in terrestrial detritus deposited in a lacustrine sediment. Org. Geochem. 3 (3), 79–89.
Deák, J., Gebhardt, A., Lewis, H., Usai, M.R., Lee, H., 2017. Soils disturbed by vegetation clearance and tillage. In: Nicosia, C., Stoops, G. (Eds.), Archaeological Soil and Sediment Micromorphology. John Wiley & Sons, Ltd, Chichester, UK, pp. 231–264.
Delvigne, J., 1998. Atlas of Micromorphology of Mineral Alteration and Weathering. Ottawa, Canada. http://petrology.oxfordjournals.org/content/41/3/475.2.short.
Duan, Y., He, J., 2011. Distribution and isotopic composition of *n*-alkanes from grass, reed and tree leaves along a latitudinal gradient in China. Geochem. J. 45 (3), 199–207.
Duan, Q., Bonn, B., Kreuzwieser, J., 2020. Terpenoids are transported in the xylem sap of Norway spruce. Plant Cell Environ. 43, 1766–1778.
Eglinton, G., Hamilton, R.J., 1967. Leaf epicuticular waxes. Science (New York, N.Y.) 156 (3780), 1322–1335.
Ejarque, A., 2013. La alta montaña pirenaica: génesis y configuración holocena de un paisaje cultural. In: Estudio paleoambiental en el valle del Madriu-Perafita-Claror (Andorra), vol. 2507. BAR International Series, Oxford.
Ejarque, A., Miras, Y., Riera, S., Palet, J.M., Orengo, H.A., 2010. Testing microregional variability in the Holocene shaping of high mountain cultural landscapes: a palaeoenvironmental case-study in the eastern Pyrenees. J. Archaeol. Sci. 37 (7), 1468–1479.
Elhmmali, M.M., Roberts, D.J., Evershed, R.P., 1997. Bile acids as a new class of sewage pollution indicator. Environ. Sci. Technol. 31 (12), 3663–3668.
Euba, I., 2008. Análisis antracológico de estructuras altimontanas en el valle de la Vansa - Sierra del Cadí (Alt Urgell) y en el valle del Madriu (Andorra): explotación de recursos forestales del Neolítico a época moderna. PhD thesis, Université de Rovira i Virgili, Tarragona, p. 358.
Euba, I., Palet, J.M., 2010. L'exploitation des ressources végétales dans les Pyrénées orientales durant l'Holocène: analyse anthracologique des structures d'élevage, de four et de charbonnières dans l'Alt Urgell (chaîne du Cadí) et la vallée du Madriu (Andorre). Quaternaire 21 (1), 305–316.
Evershed, R.P., Bethell, P.H., 1996. Application of multimolecular biomarker techniques to the identification of fecal material. In: Archaeological Soils and Sediments ACS Symposium Series, pp. 157–172.
Evershed, R.P., Bethell, P.H., Reynolds, P.J., Walsh, N.J., 1997. 5β-Stigmastanol and related 5β-stanols as biomarkers of manuring: analysis of modern experimental material and assessment of the archaeological potential. J. Archaeol. Sci. 24, 485–495.
Ficken, K.J., Li, B., Swain, D.L., Eglinton, G., 2000. An *n*-alkane proxy for the sedimentary input of the submerged/floating freshwater aquatic macrophytes. Org. Geochem. 31, 745–749.
Figueiral C., I. Carcaillet, 2005. A review of Late Pleistocene and Holocene biogeography of highland Mediterranean pines (*Pinus* tipe *sylvestris*) in Portugal, based on wood charcoal. Quat. Sci. Rev. 24, 2466–2476.
Folch, R., 1986. La vegetació del països catalans. Ketres, Barcelona.
Freeman, K.H., Pancost, R.D., 2014. Biomarkers for terrestrial plants and climate. In: Turekian, H.D., Holland, K.K. (Eds.), Treatise on Geochemistry. Elsevier, pp. 395–416.
Gabellieri, N., Pescini, V., Tinterri, D., 2020. Sulle tracce dei pastori in Liguria. In: Eredità storiche e ambientali della transumanza. Sagep, Genova.
Galop, D., 2014. Jalons pour une histoire du Pin à crochets (*Pinus uncinata* Ramond ex DC) dans les Pyrénées. In: Évaluation patrimoniale des populations autochtones de Pin à crochets (Pinus uncinata Ramond) aux Pyrénées, Collection dossiers forestiers, vol. 25, 978-2-84207-376-3.
Gassiot, E., 2016. Montañas humanizadas. Arqueología del pastoralismo en el Parque Nacional d'Aigüestortes i Estany de Sant Maurici. Organismo Autónomo Parques Nacionales, Madrid, 978-84-8014-896-2.
Gassiot, E., Rodríguez Antón, D., Burjachs, F., Antolín, F., Ballesteros, A., 2012. Poblamiento, explotación y entorno natural de los estadios alpinos y subalpinos del Pirineo central durante la primera mitad del Holoceno. Cuaternario Geomorfol. 26 (3–4), 26–42.
Gassiot, E., Rodríguez, D., Pèlachs, A., Pérez, R., Julià, R., Bal-Serin, M.C., Mazzucco, N., 2014. La alta montaña durante la Prehistoria. 10 años de investigación en el Pirineo catalán Occidental. Trab. Prehist. 71 (2), 261–281.
Gassiot, E., Mazzucco, N., Obea, L., Tarifa, N., Antolín, F., Clop, X., Navarrete, V., Saña i Seguí, M., 2015. La Cova del Sardo de Boí i l'explotació de l'alta muntanya als Pirineus occidentals en època neolítica. In: Tribuna d'Arqueologia 2012-2013, pp. 199–218.
Gassiot, E., Clemente, I., Rey, J., Obea, L., Díaz, S., Salvador, G., 2020. Dinámica de ocupación de una cueva redil del neolítico antiguo: hábitat, áreas de trabajo y estabulación en Coro Trasito (tella-Sin, Sobrarbe). In: Colegio Oficial de Doctores y Licenciados en Filosofía y letras y en Ciencias de Aragón. III Congreso de Arqueología y Patrimonio Aragonés (CAPA), pp. 29–37.
Gómez, L.O., Martínez, M.C., Huerta, R.P., Ballbè, E.G., Seijo, M.M., Baiges, G.S., Antón, D.R., Carrasco, M.Q., Mazzucco, N., Casas, D.G., Bonilla, S.D., Conte, I.C., 2021. Firewood-gathering strategies in high mountain areas of the Parc nacional d'Aigüestortes i estany de Sant maurici (central Pyrenees) during prehistory. Quat. Int. 593–594, 129–143. https://doi.org/10.1016/j.quaint.2020.11.044.
Gerasimova, M., Lebedeva, M., 2018. Organo-mineral surface horizons. In: Stoops, G., Marcellino, V., Mees, F. (Eds.), Interpretation of Micromorphological Features of Soils and Regoliths. Elsevier, Amsterdam, p. 513 538.
Greguss, P., 1959. Holzanatomie der Europäischen laubhölzer und sträucher. Helbaek, Budapest.
Guilloré, P., 1980. Méthode de fabrication mécanique et en série des lames minces, second ed. CNRS et INA-PG.
Hamerník, J., Musil, I., 2007. The *Pinus mugo* complex – its structuring and general overview of the used nomenclature. J. For. Sci. 53, 253–266.
Harrault, L., Milek, K., Jardé, E., Jeanneau, L., Derrien, M., Anderson, D.G., 2019. Faecal biomarkers can distinguish specific mammalian species in modern and past environments. PLoS One 14 (2), e0211119. https://doi.org/10.1371/journal.pone.0211119M.
IGME-Instituto Geológico y Minero de España, 1994. Geological Map at 1:50.000, Sheet Nº217 - Puigcerdá, Second Serie, first ed.
Jambrina-Enríquez, A.V., Herrera-Herrera, C., Mallol, 2018. Wax lipids in fresh and charred anatomical parts of the Celtis australis tree: insights on paleofire interpretation. Org. Geochem. 122, 147–160.
Kabukcu, C., Chabal, L., 2021. Sampling and quantitative analysis methods in anthracology from archaeological contexts: achievements and prospects. Quat. Int. 593–594, 6–18. https://doi.org/10.1016/j.quaint.2020.11.004.
Kaczorek, D., Vrydaghs, L., Devos, Y., Pető, Á., Effland, W.R., 2018. Biogenic Siliceous features. In: Stoops, G., Marcellino, V., Mees, F. (Eds.), Interpretation of Micromorphological Features of Soils and Regoliths. Elsevier, Amsterdam, pp. 157–176.
Kahmen, A., Dawson, T.E., Vieth, A., Sachse, D., 2011. Leaf wax *n*-alkane δD values are determined early in the ontogeny of Populus trichocarpa leaves when grown under controlled environmental conditions. Plant Cell Environ. 34 (10), 1639–1651.
Karkanas, P., 2010. Preservation of anthropogenic materials under different geochemical processes: a mineralogical approach. Quat. Int. 214 (1 2), 63–69.
Karkanas, P., Goldberg, P., 2018. Phosphatic features. In: Stoops, G., Marcellino, V., Mees, F. (Eds.), Interpretation of Micromorphological Features of Soils and Regoliths. Elsevier, Amsterdam, pp. 323–346.
Kooistra, M.J., Pulleman, M.M., 2018. Features related to faunal activity. In: Stoops, G., Marcellino, V., Mees, F. (Eds.), Interpretation of Micromorphological Features of Soils and Regoliths. Elsevier, Amsterdam, pp. 447–469. https://doi.org/10.1016/B978-0-444-53156-8.00018-0.
Leeming, R., Latham, V., Rayner, M., Nichols, P., 1997. Detecting and distinguishing sources of sewage pollution in Australian inland and coastal waters and sediments. Molecular Markers in Environmental Geochemistry. In: Eganhouse, R.P. (Ed.), Molecular Markers in Environmental Geochemistry. American Chemical Society, pp. 306–319.
Leierer, L., Herrera-Herrera, A.V., Jambrina-Enríquez, M., 2019. Lipid biomarker extraction and elution into different fractions from sediment. protocols.io. https://doi.org/10.17504/protocols.io.yg2ftye.
Liu, J., Liu, W., An, Z., et al., 2016. Different hydrogen isotope fractionations during lipid formation in higher plants: Implications for paleohydrology reconstruction at a global scale. Sci. Rep. 6, 19711.

Loaiza, J.C., Stoops, G., Poch, R.M., Casamijtana, M., 2015. Manual de micromorfología de suelos y técnicas complementarias, vol. 348. Fondo Editorial Pascual Bravo.
MacKenzie, W.S., Donaldson, C.H., Guilford, C., 1982. Atlas of Igneous Rocks and Their Textures. ELBS.
Macphail, R.I., Goldberg, P., 2018. Applied soils and micromorphology in archaeology. In: Barker, G., Slater, E., Bogucki, P. (Eds.), Cambridge Manuals in Archaeology. Cambridge University Press.
McParland, L., Collinson, M.E., Scott, A.C., Campbell, G., Veal, R., 2010. Is vitrification in charcoal a result of high temperature burning of wood? J. Archaeol. Sci. 37, 2679–2687.
Medeiros, P.M., Simoneit, B.R.T., 2007. Gas chromatography coupled to mass spectrometry for analyses of organic compounds and biomarkers as tracers for geological, environmental, and forensic research. J. Sep. Science 30, 1516–1536.
Nicosia, C., Stoops, G., 2017. Archaeological Soil and Sediment Micromorphology. Wiley Blackwell.
Niedermeyer, E.M., et al., 2010. Orbital- and millennial-scale changes in the hydrologic cycle and vegetation in the western African Sahel: insights from individual plant wax delta D and d13C. Quat. Sci. Rev. 29 (23–24), 2996–3005.
Niedermeyer, E.M., Forrest, M., Beckmann, B., Sessions, A.L., Mulch, A., Schefuß, E., 2016. The stable hydrogen isotopic composition of sedimentary plant waxes as quantitative proxy for rainfall in the West African Sahel. Geochem. Cosmochim. Acta 184, 55–70.
Ninot, J.M., Carrillo, E., Font, X., Carreras, J., Ferre', A., Masalles, R.M., Soriano, I., Vigo, J., 2007. Altitude zonation in the Pyrenees. A geobotanic interpretation. Phytocoenologia 37 (3–4), 371–398.
Ninot, J.M., Carrillo, E., Ferre, A., 2017. The Pyrenees. In: Loidi, J. (Ed.), The Vegetation of the Iberian Peninsula, vol. 1. Springer, M.J.A. Werger, Utrecht, The Netherlands.
Orengo, H.A., 2010. Arqueología de un paisaje cultural pirenaico de alta montaña. In: Dinámicas de ocupación del valle del Madriu-Perafita- Claror (Andorra). Ph.D. thesis. Tarragona. Rovira i Virgili University.
Orengo, H.A., Palet, J.M., Ejarque, A., Miras, Y., Riera, S., 2013. Pitch production during the Roman period: an intensive mountain industry for a globalised economy? Antiquity 87 (337), 802–814.
Orengo, H.A., Palet, J.M., Ejarque, A., Miras, Y., Riera, S., 2014a. Shifting occupation dynamics in the Madriu-Perafita-Claror valleys (Andorra) from the early Neolithic to the Chalcolithic: the onset of high mountain cultural landscapes. Quat. Int. 353, 140–152.
Orengo, H.A., Palet, J.M., Ejarque, A., Miras, Y., Riera, S., 2014b. The historical configuration of a UNESCO world heritage site: the cultural land- scape of the Madriu-Perafita-Claror Valley. Archeologia Postmedievale 17, 333–343.
Palet, J.M., Orengo, H.A., Ejarque, A., Miras, Y., Euba, I., Riera, S., 2013. Arqueología de paisajes altimontanos pirenaicos: formas de explotación y usos del medio en época romana en valle del Madriu-Perafita-Claror (Andorra) y en la Sierra del Cadí (Alt Urgell). In: Fiches, J.-L., Plana, R., Revilla, V. (Eds.), Paysages ruraux et territoires dans les cités de l'Occident romain, Actes du colloque AGER IX, pp. 329–340. Montpellier.
Palet, J.M., Garcia, A., Orengo, H.A., Riera, S., Miras, Y., Julià, R., 2014. Ocupación y explotación de espacios altimontanos pirenaicos en la antigüedad: visiones desde la arqueología del paisaje. In: Dall'Aglio, P.L., Franceschelli, C., Maganzani, L. (Eds.), Atti del IV Convegno Internazionale di Studi Veleiati. AnteQuem, Bologna, pp. 455–470.
Palet, J.M., García, A., Orengo, H.A., Polonio, T., 2017. Els espais altimontans pirenaics orientals a l'Antiguitat: 10 anys d'estudis en arqueologia del paisatge del GIAP-ICAC. Treballs arqueol. 21, 77–97.
Palet, J.M., Olmos, P., Garcia, A., Polonio, T., Orengo, H.A., 2019. Occupation et anthropisation des espaces de haute montagne dans les vallées de Nuria et Coma de Vaca (Gerona, Espagne): résultats des recherches archéologiques et patrimoniales. In: Deschamps, M., Costamagno, S., Milcent, P.Y., Pétillon, J.M., Renard, C., Valdeyron, N. (Eds.), La conquête de la montagne: des premières occupation humaines à l'anthropisation du milieu. Actes des congrès nationaux des sociétés historiques et scientifiques, Éditions du Comité des Travaux Historiques et Scientifiques. Open Edition books, Paris.
Palet, J.M., Colominas, L., Gallego-Valle, A., Martínez, J., 2020. Intervencions arqueològiques a la Capçalera del Duran i sector de Puigpedrós-Malniu (Meranges, la Cerdanya): estudi territorial d'espais altimontans pirinencs. Campanyes 2018-2019. In: Burch, J., Buxó, R., Frigola, J., Fuertes, M., Manzano, S., Mataró, M. (Eds.), Quinzenes Jornades d'Arqueologia de les Comarques de Girona(Castelló d'Empúries, Octubre 2020). Documenta Universitaria, Girona, pp. 65–70.
Padrón Herrera, H., 2021. Aproximación biomolecular y microscópica a un suelo de ocupación aborigen: La Fortaleza de Santa Lucía de Tirajana (Gran Canaria). Trabajo de Fin de Grado. Universidad de La Laguna.
Palet, J.M., Colominas, L., Carbonell, A., Gallego-Valle, A., 2022a. Intervencions arqueològiques a la Capçalera del Duran i sector de Puigpedrós-Malniu (Meranges, la Cerdanya): estudi territorial d'espais altimontans pirinencs. Campanyes 2020-2021. In: exp: 437 K121 N428 2020_1_28261/437 K121 N382 N321 N4282021-1-33064. Arqueologia dels paisatges culturals de muntanya a les capçaleres del Ter i del Segre (Ripollès-Cerdanya). Projecte Quadriennal. Generalitat de Catalunya. CLT009/18/00101).
Palet, J.M., Orengo, H.A., Garcia, A., Polonio, T., Ejarque, A., Miras, Y., Riera, S., 2022b. Landscape archaeology in eastern Pyrenees high mountain areas (Segre & ter valleys): human activities in the shaping of Mountain Cultural landscapes. In: Garcia-Molsosa, M. (Ed.), Archaeology of Mountain Landscapes: Interdisciplinary Research Strategies of Agro-Pastoralism in Upland Regions, IEMA Proceedings, vol. 12. State University of New York Press, Buffalo, pp. 179–196 (in press).
Patalano, R., Roberts, P., Boivin, N., Petraglia, M.D., Mercader, J., 2021. Plant wax biomarkers in human evolutionary studies. Evol. Anthropol. 30, 385–398.
Prost, K., Birk, J.J., Lehndorff, E., Gerlach, R., Amelung, W., 2017. Steroid biomarkers revisited - Improved source identification of faecal remains in archaeological soil material. PLoS One 12 (1), e0164882.
Quézel, P., Médail, F., 2003. Ecologie et biogéographie des forêts du bassin méditerranéen. Elsevier, Paris.
Reimer, P., Austin, W., Bard, E., Bayliss, A., Blackwell, P., Bronk Ramsey, C., Talamo, S., et al., 2020. The IntCal20 northern hemisphere radiocarbon age calibration curve (0–55 cal kBP). Radiocarbon 62 (4), 725–757. https://doi.org/10.1017/RDC.2020.41.
Rendu, C., 2003. La montagne d'Enveig. Une estive pyrénéenne dans la longue durée. Canet, Trabucaire Editions.
Rojo Guerra, M.A., Pena-Chocarro, L., Royo-Guillen, J.I., Tejedor Rodríguez, C., García Martínez de Lagran, I., Arcusa Magallón, H., Garrido Pena, R., Moreno-García, M., Mazzucco, N., Gibaja Bao, J.F., Ortega, D., Kromer, B., Alt, K.W., 2013. Pastores trashumantes del Neolítico Antiguo en un entorno de alta montãna: secuencia crono-cultural de la Cova de Els Trocs (San Feliú de Veri, Huesca). In: Carnicero, F.R. (Ed.), Boletin del seminario de estudios de arte y araqueologia. Universidad de Valladolid, Valladolid, pp. 9–55.
Rojo Guerra, M.A., Arcusa Magalóon, H., Pe~na-Chocarro, L., Royo Guillén, J.I., Tejedor Rodríguez, C., García Martínez de Lagrán, I., Garrido Pena, R., Moreno García, M., Pimenta, C., Mazzucco, N., Gibaja Bao, J.F., Pérez Jordà, G., Jiménez Jiménez, I., Iriarte, E., Alt, K.W., 2014. Los primeros pastores transhumantes de la Alta Ribagorza. In: Clemente, I., Gassiot Ballb, e E., Rey Lanaspa, J. (Eds.), Sobrarbe antes de Sobrarbe: pinceladas de historia de los Pirineos. Centro de Estudios de Sobrarbe, Instituto de Estudios Altoaragoneses, pp. 127–151.
Sachse, D., Radke, J., Gleixner, G., 2006. δD values of individual *n*-alkanes from terrestrial plants along a climatic gradient – Implications for the sedimentary biomarker record. Org. Geochem. 37 (4), 469–483.
Schäfer, I.K., Lanny, V., Franke, J., Eglinton, T.I., Zech, M., Vysloužilová, B., Zech, R., 2016. Leaf waxes in litter and topsoils along a European transect. SOIL 2, 551–564.
Schemmel, F., Niedermeyer, E.M., Schwab, V.F., Gleixner, G., Pross, J., Mulch, A., 2016. Plant wax δD values record changing Eastern Mediterranean atmospheric circulation patterns during the 8.2 kyr B.P. climatic event. Quat. Sci. Rev. 133, 96–107.
Schlanser, K.M., Diefendorf, A.F., West, C.K., Greenwood, D.R., Basinger, J.F., Meyer, H. W., Lowe, A.J., Naake, H.H., 2020. Conifers are a major source of sedimentary leaf wax *n*-alkanes when dominant in the landscape: case studies from the Paleogene. Org. Geochem. 147, 104069.
Schweingruber, F.H., 1990. Anatomy of European Woods. Haupt, Stuttgart.
Shahack-Gross, R., 2017. Animal gathering enclosures. In: Nicosia, C., Stoops, G. (Eds.), Archaeological Soil and Sediment Micromorphology. John Wiley & Sons, Ltd, pp. 265–280.
Shillito, L.M., Bull, I.D., Matthews, W., Almond, M.J., Williams, J.M., Evershed, R.P., 2011. Biomolecular and micromorphological analysis of suspected faecal deposits at Neolithic Çatalhöyük, Turkey. J. Archaeol. Sci. 38 (8), 1869–1877.
Sokołowska, J., Fuchs, H., Celiński, K., 2021. New insight into taxonomy of European mountain pines, Pinus mugo complex, based on complete chloroplast genomes sequencing. Plants 10 (7), 1331. https://doi.org/10.3390/plants10071331.
Stoops, G., 2021. Guidelines for Analysis and Description of Soil and Regolith Thin Sections. Second Edition. Soil Science Society of America, 184, John Wiley & Sons.
Stoops, G., Mees, F., 2018. Groundmass composition and fabric. In: Stoops, G., Marcellino, V., Mees, F. (Eds.), Interpretation of Micromorphological Features of Soils and Regoliths. Elsevier, Amsterdam, pp. 73–125.
Stoops, G., Schaefer, C.E.G.R., 2018. Pedoplasmation: formation of soil material. In: Stoops, G., Marcellino, V., Mees, F. (Eds.), Interpretation of Micromorphological Features of Soils and Regoliths. Elsevier, Amsterdam, pp. 59–71.
Stoops, G., Marcelino, V., Mees, F. (Eds.), 2018. Interpretation of Micromorphological Features of Soils and Regoliths. Elsevier.
Tejedor-Rodríguez, C., Moreno-García, M., Tornero, C., Hoffmann, A., García-Martínez, I., Arcusa-Magallón, H., garrido-Pena, R., Royo-Guillén, J.-I., Díaz-Navarro, S., Peña-Chocarro, L., Alt, K., Rojo-Guerra, M., 2020. Investigating neolithic caprine husbandry in the central Pyrenees: insights from a multi-proxy study at Els Trocs cave (Bisaurri, Spain). PLoS One 16 (1), e0244139. https://doi.org/10.1371/journal.pone.0244139.
Tomé, L., Jambrina-Enríquez, M., Égüez, N., et al., 2022. Fuel sources, natural vegetation and subsistence at a high-altitude aboriginal settlement in Tenerife, Canary Islands: microcontextual geoarchaeological data from Roques de García Rockshelter. Archaeol Anthropol Sci 14, 195.
Tornero, C., Aguilera, M., Ferrio, J.P., Arcusa, H., Moreno-García, M., Garcia-Reig, S., Rojo-Guerra, M., 2016. Vertical sheep mobility along the altitudinal gradient through stable isotope analyses in tooth molar Bioapatite, meteoric water and pastures: a reference from the ebro valley to the central Pyrenees. Quat. Int. 484, 94–106. https://doi.org/10.1016/j.quaint.2016.11.042.
Vepraskas, M.J., Lindbo, D.L., Stolt, M.H., 2018. Redoximorphic features. In: Stoops, G., Marcellino, V., Mees, F. (Eds.), Interpretation of Micromorphological Features of Soils and Regoliths. Elsevier, Amsterdam, p. 425 445.
Verrecchia, E.P., Trombino, L., 2021. A Visual Atlas for Soil Micromorphologists. Springer International Publishing, p. 184.
Vidaković, M., 1991. Conifers: morphology and variation. Graficki Zavod.
Vigo, J., 2009. L'Alta Muntanya Catalana: Flora I Vegetació, 2nd revised Ed. (Barcelona).
Walsh, K., Court-Picon, M., Beaulieu, J.-L., Guiter, F., Mocci, F., Richer, S., Sinet, R., Talon, B., Tzortzis, S., 2014. A historical ecology of the Ecrins (southern French Alps): archaeology and palaeoecology of the Mesolithic to the Medieval period. Quat. Int. 353 (5), 52–73.

Web references

http://www.woodanatomy.ch. (Accessed 5 February 2022).
https://insidewood.lib.ncsu.edu. (Accessed 5 February 2022).
https://www.wsl.ch/dendropro/xylemdb. (Accessed 5 February 2022).
https://www.plantatlas.eu. (Accessed 4 July 2022).
http://www.theplantlist.org. (Accessed 12 June 2022).
https://www.biologydiscussion.com/gymnosperm/pinus-external-morphology-and-different-parts/33923. (Accessed 10 April 2022).